

**N 8 4 - 2 3 6 2 1**

## **NASA Contractor Report 172321**

**APPLICATION OF NEAR-TERM TECHNOLOGY TO A MACH 2.0  
VARIABLE-SWEEP-WING, SUPERSONIC-CRUISE EXECUTIVE JET**

**F. L. Beissner, Jr., W. A. Lovell, A. Warner Robins,  
and E. E. Swanson**

**Kentron International, Inc.  
Aerospace Technologies Division  
Hampton, Virginia 23666**

**Contract NAS1-16000  
March 1984**

**NASA**  
National Aeronautics and  
Space Administration  
**Langley Research Center  
Hampton, Virginia 23665**

## SUMMARY

A study has been conducted to assess the impact of variable-sweep-wing technology with relaxed static stability requirements on a supersonic-cruise executive jet with transatlantic range. The baseline concept utilizes superplastic formed/diffusion bonded titanium structural concepts and modified current technology engines and meets the supersonic-cruise Mach number requirements while providing excellent low-speed characteristics. Advanced composite structural concepts and alternate engines were also evaluated as were alternate flight profiles for reduced sonic-boom overpressures during overland flight.

The baseline concept has a ramp weight of 64,500 pounds with a crew of two and eight passengers. Its Mach 2.0 cruise range is nearly 3,500 nautical miles, and its Mach 0.9 cruise range is over 5,000 nautical miles. Takeoff, landing, and balanced field length requirements were calculated for a composite variant and are all less than 5,000 feet.

## INTRODUCTION

Variable-sweep wings have been proposed for use on supersonic-cruise civil aircraft due to conflicting requirements at low and high speeds. At low speeds, wings with low sweep and high span provide performance compatible with airport requirements; wings with high sweep and long lifting surfaces have good efficiency for the supersonic cruise conditions. Early variable-sweep, civil designs (ref. 1 through 4) were adversely affected by the need to maintain static longitudinal stability throughout the operating envelope. This stability reached high levels at cruise due to rearward shifts in the aerodynamic center with increases in both wing sweep and Mach number. Although the adverse effects of wing sweep were reduced by the introduction of outboard wing hinges, the large wing gloves associated with these hinges tend to produce severe low-speed nonlinearities in pitch characteristics. This problem required the linearizing effects of a low horizontal tail. The hostile acoustical and thermal environment for the low tail, due to the presence of the jet exhausts, led to the introduction of the compound wing/horizontal-tail concept with the tail-mounted engines. This last concept, however, had severe aeroelasticity problems.

The application of variable-sweep concepts to supersonic-cruise civil aircraft now appears more feasible due to developments in stability and control technology. Relaxed static longitudinal stability is utilized on several high-speed aircraft, even in vehicles with limited longitudinal control power (such as the Concorde). This paper reports on the application of such technologies to the conceptual development of a supersonic executive jet. Mission requirements are for a vehicle to carry eight passengers at not less than Mach 2.0 with a transatlantic range. References 5 and 6 report the results of studies of fixed-wing concepts designed to meet similar requirements.

## REFERENCES

1. The Boeing Company Airplane Division: Phase I Comprehensive Report, Commercial Supersonic Transport Program. January 1964.
2. The Boeing Company Airplane Division: Phase IIA Comprehensive Report, Commercial Supersonic Transport Program. November 1964.

3. The Boeing Company Airplane Division: Phase IIC Comprehensive Report, Commercial Supersonic Transport Program. November 1965.
4. The Boeing Company Airplane Division: Phase III Comprehensive Report, Commercial Supersonic Transport Program. September 1966.
5. DaCosta, Roy. A.; Espil, G. J.; Everest, D. L.; Lovell, W. A.; Martin, Glenn L.; Swanson, E. E.; and Walkley, K. B.: Concept Development Studies for a Mach 2.7 Supersonic-Cruise Business Jet. NASA CR-165705, April 1981.
6. Beissner, F. L., Jr.; Lovell, W. A.; Robins, A. Warner; and Swanson, E. E.: Effect of Advanced Technology and a Fuel Efficient Engine on a Supersonic Cruise Executive Jet with a Small Cabin. NASA CR-172190, August 1983.

## SYMBOLS

a.c.	aerodynamic center
$A_x$	cross-section area
$\bar{c}$	mean geometric chord
c.g.	center-of-gravity location
$C_D$	drag coefficient, $\frac{(\text{Drag})}{qS}$
$\Delta C_{D_{\text{GEAR}}}$	drag coefficient increment for landing gear
$C_L$	lift coefficient $\frac{(\text{Lift})}{qS}$
$C_m$	pitching-moment coefficient $\frac{(\text{pitching-moment})}{qS\bar{c}}$
$C_{m_0}$	zero-lift pitching-moment coefficient
$\frac{\partial C_m}{\partial C_L}$	longitudinal stability parameter, percent $\bar{c}$
h	altitude
KCAS	calibrated airspeed in knots
L/D	lift-drag ratio ( $C_L/C_D$ )
M	Mach number
$\Delta p$	sonic-boom overpressure
q	freestream dynamic pressure
S	wing reference area
W	aircraft weight
x, y, z	Cartesian coordinates
$\alpha$	angle of attack
$\delta$	deflection angle of movable surface, normal to hinge line
$\Lambda$	wing sweep angle

### Subscripts:

f	friction
F	wing flap
H	horizontal tail

L.E.	leading edge
max	maximum
o	zero-lift condition
R	roughness
TE	trailing edge
W	wave

## PART I. - CONCEPT DEVELOPMENT

A. W. Robins

The first step in the evolution of the concept configuration was the definition of a representative geometry and the calculation of the associated stability and trim characteristics. A more detailed configuration definition was subsequently developed with emphasis on aerodynamic performance at high speed. Aeroelastic effects, although very important to a full-fledged design effort, are not likely to alter feasibility and are beyond the scope of this study.

### Stability and Trim Considerations

The primary objective of the concept development was for the aircraft to be essentially self-trimming throughout most of its operating envelope, using only wing sweep and wing trailing-edge flaps. Horizontal-tail deflection is thereby reserved largely for longitudinal control, particularly at the heavier weight conditions.

The operational concept of the study aircraft depends upon the variable-stability nature of variable sweep as portrayed in figure I-1, which shows the effects of wing sweep and Mach number on rigid-aircraft, static longitudinal stability. The subsonic and transonic values shown were obtained using the methods of references I-1 and I-2 adjusted according to the data of references 3 and 4 of the Introduction. Supersonic values were obtained using the method of references I-3, I-4, I-5, and I-6. The moment center for this figure corresponds to the center of gravity of the aircraft at maximum takeoff gross weight. The configuration is seen to be statically unstable longitudinally at the lower angles of wing sweep -- a design condition not permitted during the development of the variable sweep concepts of the National Supersonic Transport program. This static instability permits trimming the aircraft with downward flap deflection. Zero-lift pitching-moment increments at 20 and 30 degrees of sweep and for various flap deflections were calculated by the method of reference I-7, and corrected to reflect the tail-on condition and the nonlinearities seen at the higher flap deflections in the experimental data of reference 3 of the Introduction. The supersonic values were obtained by the method of references I-3 through I-6. Figure I-2 shows some values taken from figure I-1 plotted as the pitching-moment

curves corresponding to takeoff at maximum gross weight, landing at maximum landing weight, and the begin-cruise condition. In each of these three cases the configuration is trimmed at zero tail deflection and at a center-of-gravity location corresponding to that for takeoff at maximum gross weight. Flap deflections of  $15^\circ$ ,  $40^\circ$ ,  $-1^\circ$ , and wing sweep angles of  $27.3^\circ$ ,  $20^\circ$ , and  $68^\circ$  are required for the takeoff, landing, and begin-cruise conditions, respectively.

In contrast to the fixed center-of-gravity cases shown to this point, optimizing the overall wing/tail geometry for a given flight condition will require use of the variable center-of-gravity feature (programmed fuel utilization) of the aircraft. Figure I-3 shows the center-of-gravity envelopes and the rigid-aircraft aerodynamic centers for the three conditions called out in figure I-2. The three points denote those constant center-of-gravity conditions for takeoff, landing, and supersonic cruise previously shown. At the lightest landing weights, even at the most aft center-of-gravity condition, the aircraft will be neutrally or positively stable, requiring some horizontal-tail deflection for trim. At the supersonic-cruise condition, the aircraft is seen to be statically stable at all weights. To optimize configuration geometry for this critical condition, aft movement of the center-of-gravity is necessary. When done in conjunction with a wing-flap deflection of  $-4.25$  degrees (which provides both improved trimming moment and what will subsequently be shown to be lower drag), this will permit trimming the aircraft at a drag-reducing tail-deflection of  $+2.0$  degrees (see section V of reference 5 of the Introduction). Figure I-4 shows pitching moment versus lift coefficient at this reduced-stability condition and shows the effects of both flap and tail deflections. These and the supersonic drag-due-to-lift values (to be subsequently shown) were calculated using the method of references I-3 through I-6.

#### Wing Camber and Twist Considerations

Subsonic performance considerations led to the choice of derivatives of the refined NASA supercritical airfoils of references I-8 and I-9 at  $20$  degrees of sweep. At  $68$  degrees sweep, decambering of the resulting airfoil sections by upward deflection of the wing flaps resulted in improvements in induced drag as seen in figure I-5.

In developing the cruise shape of the wing, wing twist was exercised using the method of references I-3 through I-6. With the reduced stability (and an attendant



reduced trimming-moment requirement) and with the blunt leading edges swept well behind the Mach line, a mild twist distribution (a wash-out of just over 3 degrees) was selected. Figure I-5 shows, however, that the selected geometry very nearly achieves the ideal of full leading-edge thrust, combining the distributed thrust arising from camber and twist with significant amounts of leading-edge thrust (see ref. I-10).

### Wave Drag Optimization

Once the lifting system was defined, the remaining components were assembled to retain the drag-due-to-lift characteristics of the lifting system while substantially reducing configuration wave drag. The largest-volume item, the fuselage, was integrated in the supersonic lifting system by providing that its rate of change of cross-section area above and below the wing camber surface be equal (see refs. I-11 and I-12). In the optimization of supersonic wave drag, a far-field analysis method described in reference I-13 was utilized. A feature of the program is an ability to define a least-drag fuselage area-distribution through a set of constraining fuselage stations in a given assemblage of components and for a given Mach number. This feature was utilized after careful tailoring was employed to alleviate sharp local changes in area development such as at the junction of the thick upper elements of the vertical tail and the horizontal tail or at the empennage/body juncture. The empennage pod and dorsal fins are results of such tailoring. The final fuselage area distribution with the specified constraint stations is shown in figure I-6. The Mach-2.0 average-equivalent-body area distribution, with the contributions of the various configuration components indicated, is shown in figure I-7. The numerical model of the complete configuration in the format of reference I-14 is shown in table I-I. A computer drawing of this modeling is shown as figure I-8.

### REFERENCES

- I-1. Paniszczyn, Thomas F.: Prediction of Lift and Aerodynamic Center for Variable-Sweep Wings. AIAA Paper No. 67-135. January 23-26, 1967.
- I-2. British Data Sheets: Item 70011 with Amendment C, July 1977.

- I-3. Middleton, W. D.; and Lundry, J. L.: A System for Aerodynamic Design and Analysis of Supersonic Aircraft. Part 1 - General Description and Theoretical Development. NASA CR 3351, December 1980.
- I-4. Middleton, W. D.; and Lundry, J. L.: A System for Aerodynamic Design and Analysis of Supersonic Aircraft. Part 2- User's Manual. NASA CR 3352, December 1980.
- I-5. Middleton, W. D.; and Lundry, J. L.: A System for Aerodynamic Design and Analysis of Supersonic Aircraft. Part 3 - Computer Program Description. NASA CR 3353, December 1980.
- I-6. Middleton, W. D.; and Lundry, J. L.: A System for Aerodynamic Design and Analysis of Supersonic Aircraft. Part 4 - Test Cases. NASA CR 3354, December 1980.
- I-7. Carlson, Harry W.; and Walkley, Kenneth B.: An Aerodynamic Analysis Computer Program and Design Notes for Low Speed Wing Flap Systems. NASA Contractor Report 3675, March 1983.
- I-8. Harris, Charles D.: Aerodynamic Characteristics of the 10-Percent-Thick NASA Supercritical Airfoil 33 Designed for a Normal-Force Coefficient of 0.7. NASA TM X-72711, 1975.
- I-9. Harris, Charles D.: Aerodynamic Characteristics of a 14-Percent-Thick NASA Supercritical Airfoil Designed for a Normal-Force Coefficient of 0.7. NASA TM X-72712, 1975.
- I-10. Carlson, Harry W.; Mack, Robert J.; and Barger, Raymond L.: Estimation of Attainable Leading-Edge Thrust for Wings at Subsonic and Supersonic Speeds. NASA TP 1500, October 1979.
- I-11. Baals, D. D.; Robins, A. W.; and Harris, R. V., Jr.: Aerodynamic Design Integration of Supersonic Aircraft. J. Airc., Vol. 7, No. 5, Sept.-Oct. 1970, pp. 385-394.

- I-12. Dollyhigh, Samuel; and Morris, Odell A.: Experimental Effects of Fuselage Camber on Longitudinal Aerodynamic Characteristics of a Series of Wing-Fuselage Configurations at a Mach Number of 1.41. NASA TM X-3411, 1976.
- I-13. Harris, Roy V., Jr.: An Analysis and Correlation of Aircraft Wave Drag. NASA TM X-947, 1964.
- I-14. Craidon, Charlotte B.: Description of a Digital Computer Program for Airplane Configuration Plots. NASA TM X-2074, 1970.

TABLE I-1. - NUMERICAL MODEL OF COMPLETE CONFIGURATION.

SXJT130, ENLARGED AFT FUSE, S=690, L=107, 1120, ENG, SWEEP#68, 12/03																	
1	1	1	1	1	6	20	1	14	30	2	15	2	10	2	10	REF	SCX
690.0	19.79	58.118															XAF 1
0.	5.	2.0	5.0	10.0	15.0	20.0	25.0	30.0	40.0								XAF 2
50.0	60.0	65.0	70.0	75.0	80.0	85.0	90.0	95.0	100.0								WAFORC1
31.219	2.9167	2.646	24.1209														WAFURU2
37.737	5.5500	2.154	21.8453														WAFURU3
48.854	9.9609	1.811	18.0344														WAFURU4
58.851	14.0	1.701	14.5447														WAFURU5
64.927	16.535	1.671	12.3543														WAFURU6
72.512	19.6	1.727	2.0043														WAFURU7
U.	.0163	.0493	.1013	.1743	.2446	.3130	.3774	.4478	.5766								IZURU1A
U.	.0463	.0000	.0859	.0618	.0822	.0955	.0470	-1.0243	-1.1762	-1.4150							IZURU1B
U.	.0125	.0342	.0650	.1045	.1415	.1766	.2105	.2450	.3080								IZURU2A
U.	.3621	.4023	.4076	.4040	.3451	.3889	.3441	.4471	.5540	.7421							IZURU2B
U.	.0133	.0248	.0382	.0524	.0651	.0762	.0854	.0946	.1115								IZURU3A
U.	.1193	.1167	.1079	.0916	.0743	.0584	.0561	.0773	.1405	.2557							IZURU3B
U.	.0100	.0137	.0184	.0228	.0251	.0265	.0284	.0283	.0285								IZURU4A
U.	.0243	.0120	.0015	.0187	.0358	.0914	.0585	.0461	.0033	.0846							IZURU4B
U.	.0043	.0043	.0057	.0076	.0071	.0067	.0062	.0043	.0014	.0035							IZURU5A
U.	.0109	.0233	.0342	.0492	.0691	.0745	.0865	.0804	.0454	.0262							IZURU5B
U.	.0001	.0003	.0007	.0013	.0020	.0027	.0033	.0040	.0053								IZURU6A
U.	.0007	.0080	.0087	.0093	.0100	.0107	.0113	.0120	.0127	.0133							IZURU6B
U.	.4610	.8623	1.2570	1.5437	1.8126	1.9883	2.1243	2.2238	2.3300								WAFURU1A
U.	2.3333	2.1708	1.9434	1.7330	1.4311	1.0882	.7280	.4162	.1824	0.0							WAFURU1B
U.	.4669	.8716	1.2726	1.6132	1.8347	2.0123	2.1497	2.2522	2.3584								WAFURU2A
U.	2.3621	2.1963	2.0068	1.7542	1.4484	1.1005	.7379	.4211	.1850	0.0							WAFURU2B
U.	.5212	.9826	1.4018	1.7610	1.9828	2.1354	2.2513	2.3040	2.3406								WAFURU3A
U.	2.2513	2.0117	1.8121	1.5614	1.2754	.9557	.6343	.3682	.1547	0.0							WAFURU3B
U.	.5060	.9268	1.3146	1.6611	1.8701	2.0186	2.1258	2.1836	2.2029								WAFURU4A
U.	2.1258	1.8949	1.7023	1.4741	1.2128	.9150	.6100	.3465	.1513	0.0							WAFURU4B
U.	.4759	.8839	1.2466	1.5735	1.7710	1.9038	2.0010	2.0624	2.0831								WAFURU5A
U.	2.0042	1.7472	1.6124	1.3982	1.1526	.8710	.5925	.3400	.1392	0.0							WAFURU5B
U.	.00001	.00002	.00003	.00004	.00005	.00006	.00007	.00008	.00009								WAFURU6A
U.	.00010	.00009	.00008	.00007	.00006	.00005	.00004	.00002	.00001	0.0							WAFURU6B
U.	.3.69	7.38	11.07	14.76	18.45	22.14	25.83	29.52	33.21								XFUS 10
U.	36.90	40.59	44.28	47.97	51.66	55.35	59.04	62.73	66.42	70.11							XFUS 20
U.	73.80	77.49	81.18	84.87	88.56	92.25	95.94	99.63	103.32	107.01							XFUS 30
U.	2.690	2.815	2.940	3.115	3.420	3.754	3.880	3.840	3.725	3.510							ZFUS 10
U.	3.220	2.960	2.535	2.160	1.790	1.435	1.122	.870	.670	.530							ZFUS 20
U.	.425	.350	.295	.270	.250	.230	.220	.210	.200	.190							ZFUS 30
U.	0.0	2.294	6.434	11.3	16.360	21.867	26.663	29.442	29.384	27.463							AFUS 10
U.	24.4	21.48	20.36	21.62	22.04	21.88	21.70	21.73	21.80	21.62							AFUS 20
U.	20.68	19.45	17.33	14.14	11.21	8.98	5.80	2.60	.92	0.0							AFUS 30
U.	100.10	0.0	7.584														PFUURU 1
U.	0.0	1.0	2.0	3.0	4.0	5.012	5.2	5.4	5.6	5.8							XFUU 1=1
U.	6.0	6.3	6.7	7.1	7.6												XFUU 1=2
U.	0.0	.154	.272	.353	.402	.420	.415	.402	.381	.344							PFUR 1=1
U.	.355	.262	.145	.071	0.0												PFUR 1=2
U.	48.5	5.80	-1.70														WAFURU
U.	0.0	2.0	4.0	5.5	7.0	8.368	9.5	10.5	12.0	13.343							XFUUA
U.	16.301	17.468	18.0	19.5	19.401												XFUUB
U.	1.404	1.429	1.453	1.471	1.440	1.507	1.521	1.533	1.551	1.568							PFUUA
U.	1.604	1.604	1.604	1.604	1.604												PFUUB
U.	79.033	0.0	1.50	26.064	99.277	0.0	3.00	11.107									FNURU 1
U.	0.0	10.0	20.0	30.0	40.0	50.0	60.0	70.0	80.0	90.0	100.0						XFAN 1
U.	0.0	.230	.430	.588	.697	.748	.744	.749	.532	0.0							FNURU1=1
U.	0.0	.518	.941	1.267	1.498	1.633	1.672	1.555	.719	0.0							FNURU1=2
U.	95.277	0.0	3.00	11.107	105.1130.0	7.544	5.213										FNURU 2
U.	0.0	10.0	20.0	30.0	40.0	50.0	60.0	70.0	80.0	90.0	100.0						XFAN 2
U.	0.0	.518	.941	1.267	1.498	1.633	1.672	1.555	.719	0.0							FNURU2=1
U.	0.0	.918	1.669	2.251	2.667	2.917	3.000	2.814	1.517	0.0							FNURU2=2
U.	47.2	1.92	.28	23.3	50.0	4.30	-1.33	17.0									SIRURU
U.	0.0	20.0	30.0	40.0	50.0	60.0	70.0	80.0	90.0	100.0							XIRU1
U.	0.0	1.28	1.68	1.92	2.00	1.94	1.88	1.88	.72	0.0							SIRURU
U.	0.0	1.28	1.68	1.92	2.00	1.92	1.88	1.88	.72	0.0							SIRURU
U.	105.13	0.0	7.594	10.049	114.42	5.652	7.544	2.512									MIURU
U.	0.0	10.0	20.0	30.0	40.0	50.0	60.0	70.0	80.0	90.0	100.0						XMIAL
U.	0.0	.533	.948	1.264	1.448	1.500	1.448	1.264	.533	0.0							MIURU
U.	0.0	.533	.948	1.264	1.448	1.500	1.448	1.264	.533	0.0							MIURU

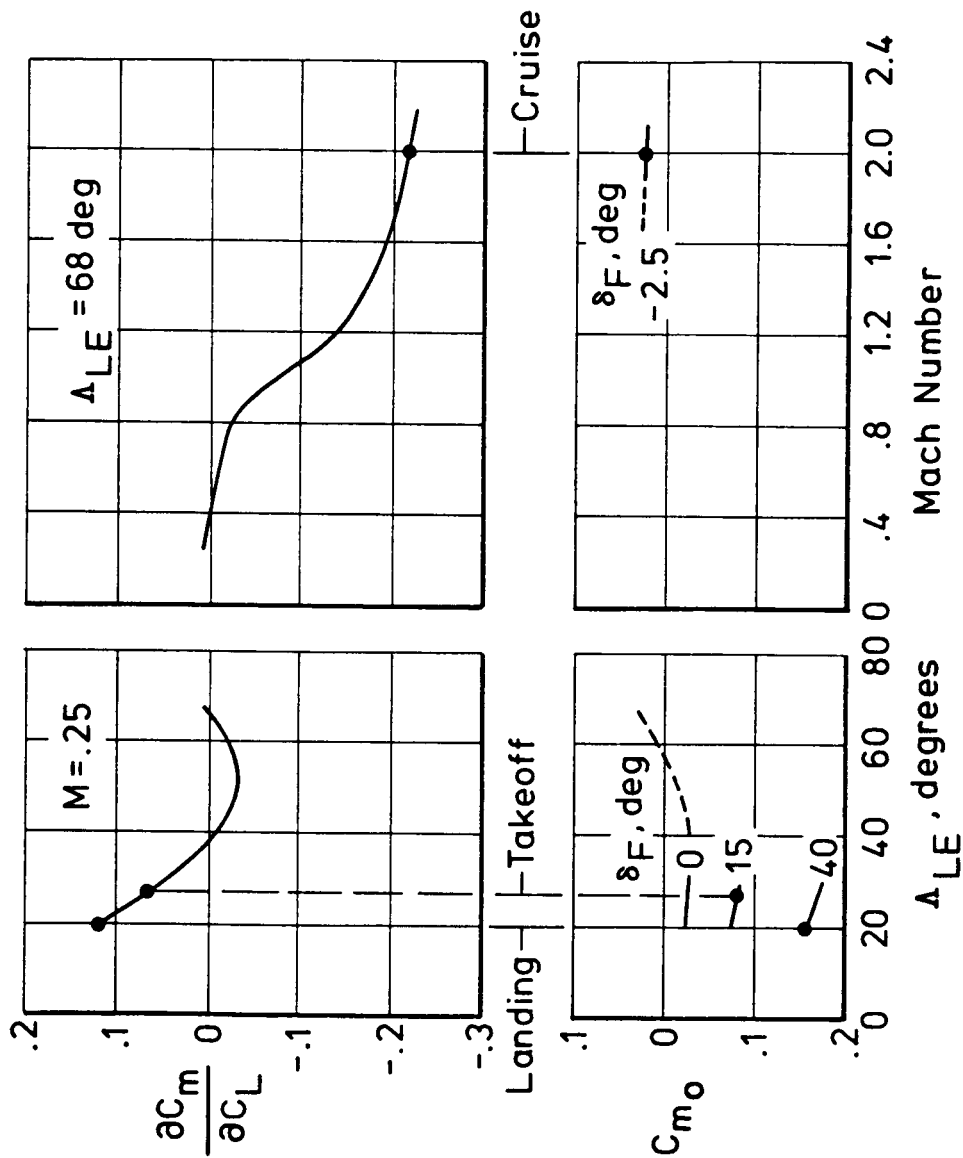


Figure I-1. - Effects of wing sweep and Mach number on the static longitudinal stability and zero-lift pitching-moment characteristics. Moment center is at the center of gravity for maximum gross weight.  $\delta_H = 0^\circ$

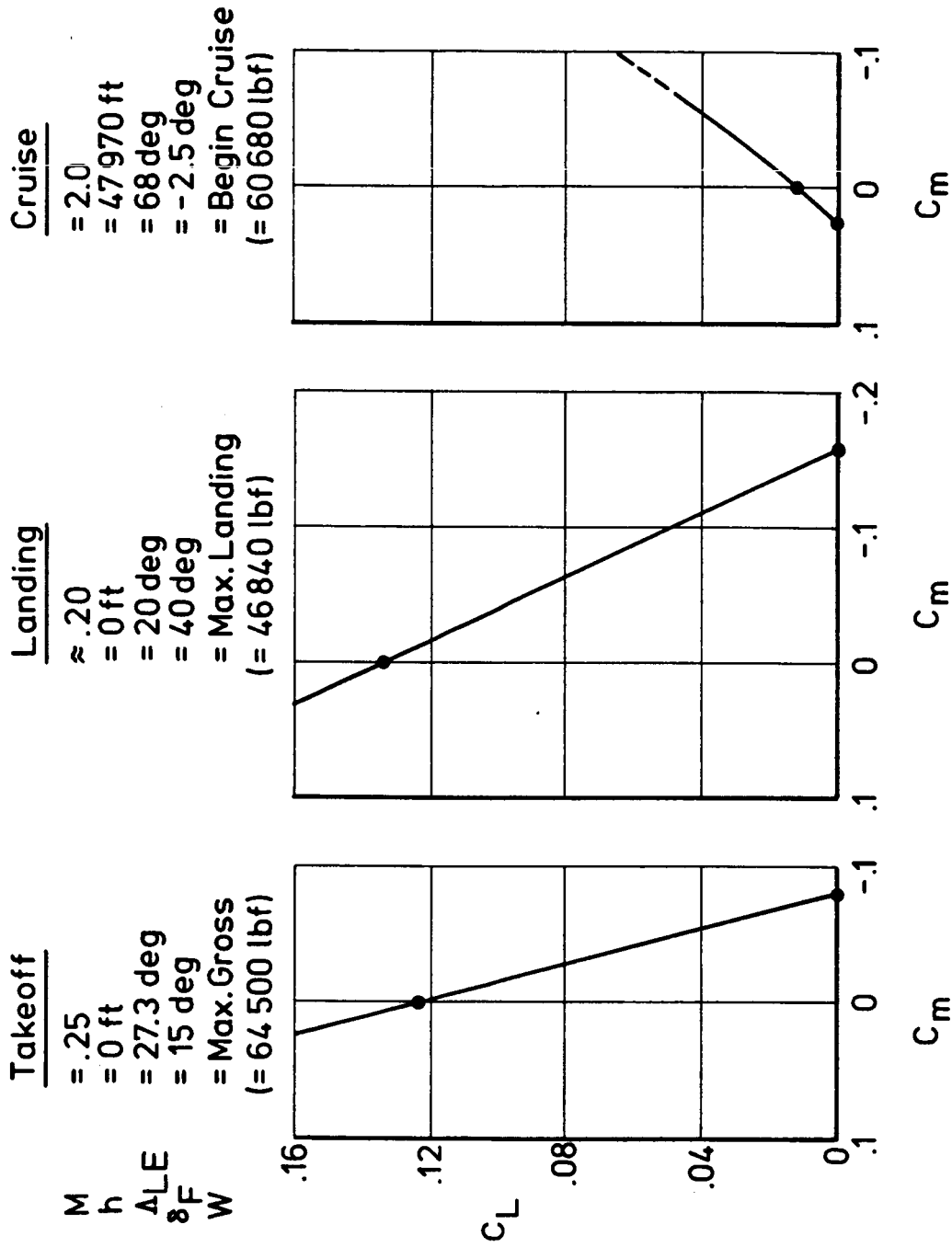


Figure I-2. - Stability and trim conditions. Horizontal-tail deflection = 0°; and center-of-gravity for maximum gross weight (.683c̄).

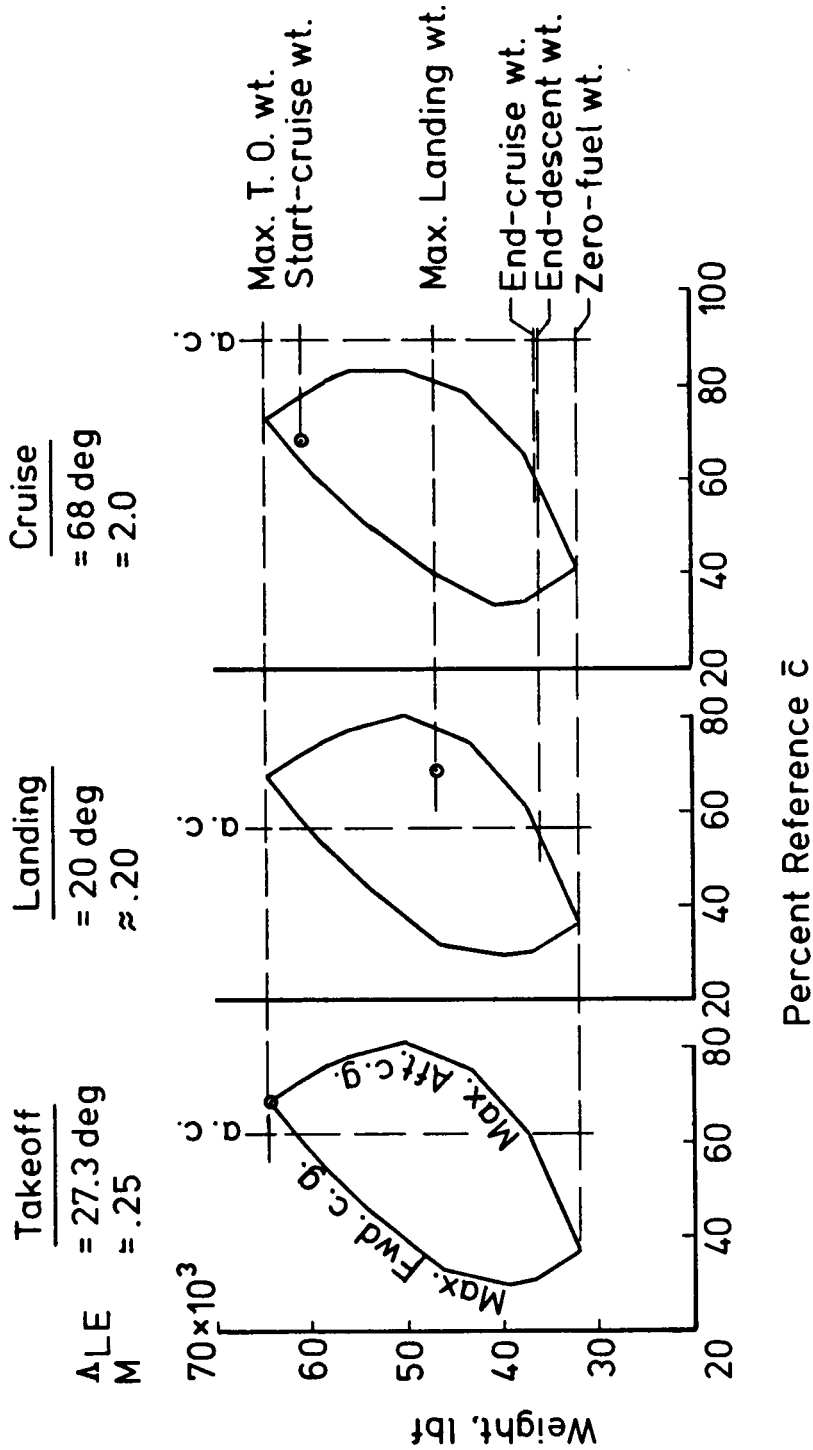


Figure I-3. - Center of gravity (c.g.) and rigid-aircraft aerodynamic center (a.c.) locations at wing sweep angles for takeoff, landing, and supersonic cruise. Points correspond to conditions of figure I-2.

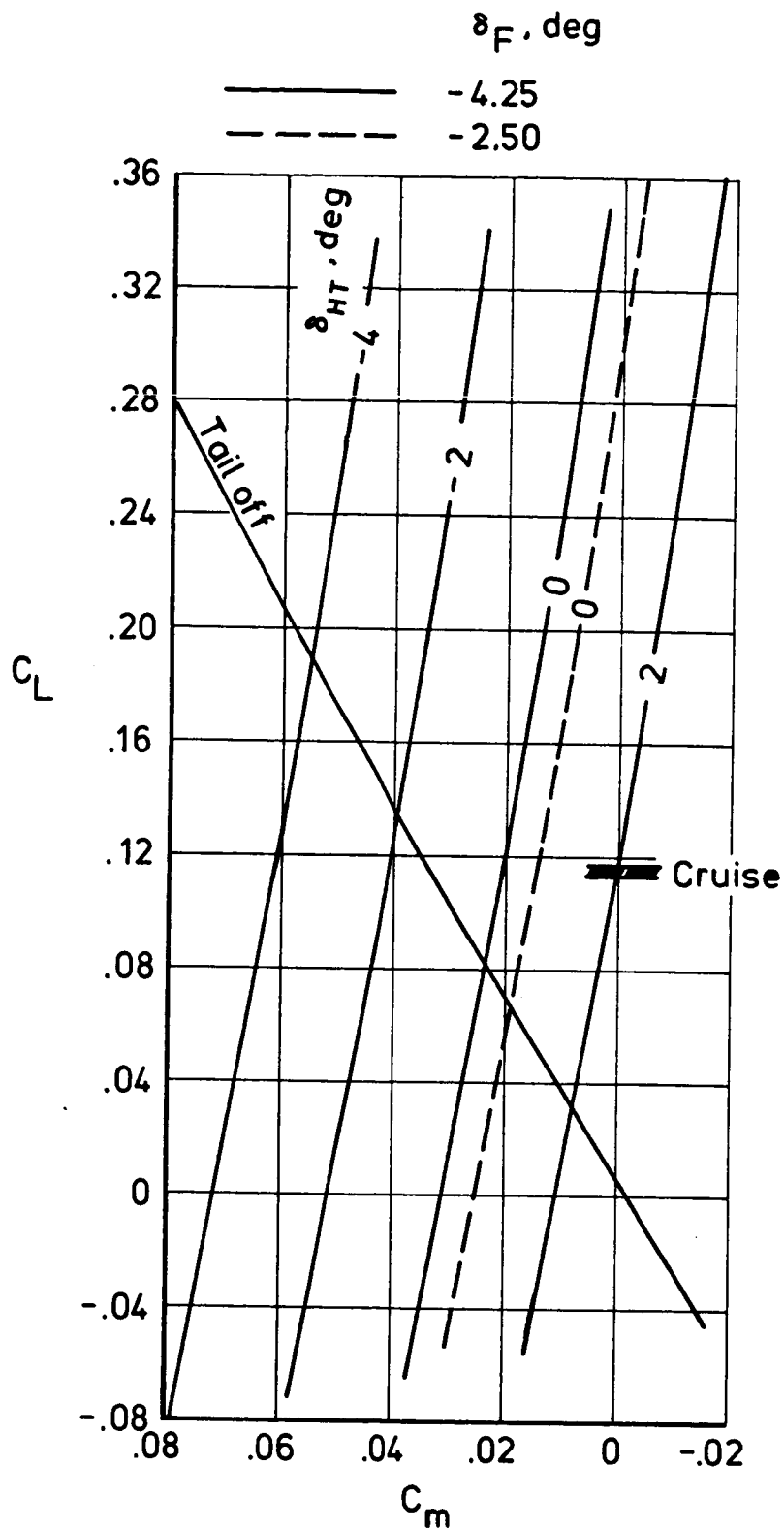


Figure I-4. - Effects of wing flaps and horizontal tail on trim characteristics at reduced stability.  $M = 2.0$ ; and center-of-gravity at  $.80\bar{c}$ .



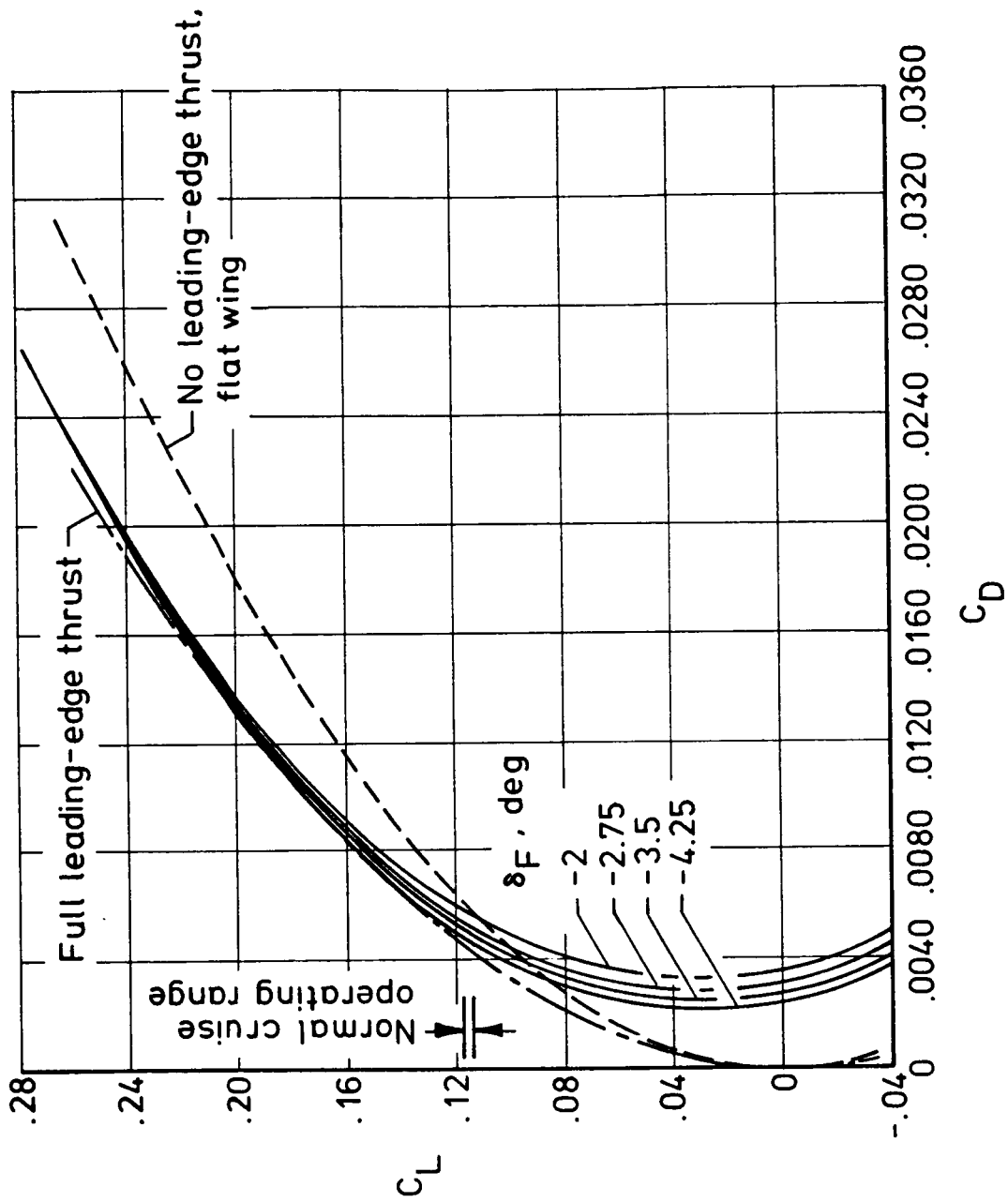


Figure I-5. - Drag due to lift of complete aircraft at  $M = 2.0$  and  $\delta\mu = 0^\circ$  as affected by wing flap deflections.  $\Lambda_{LE} = 68^\circ$ .

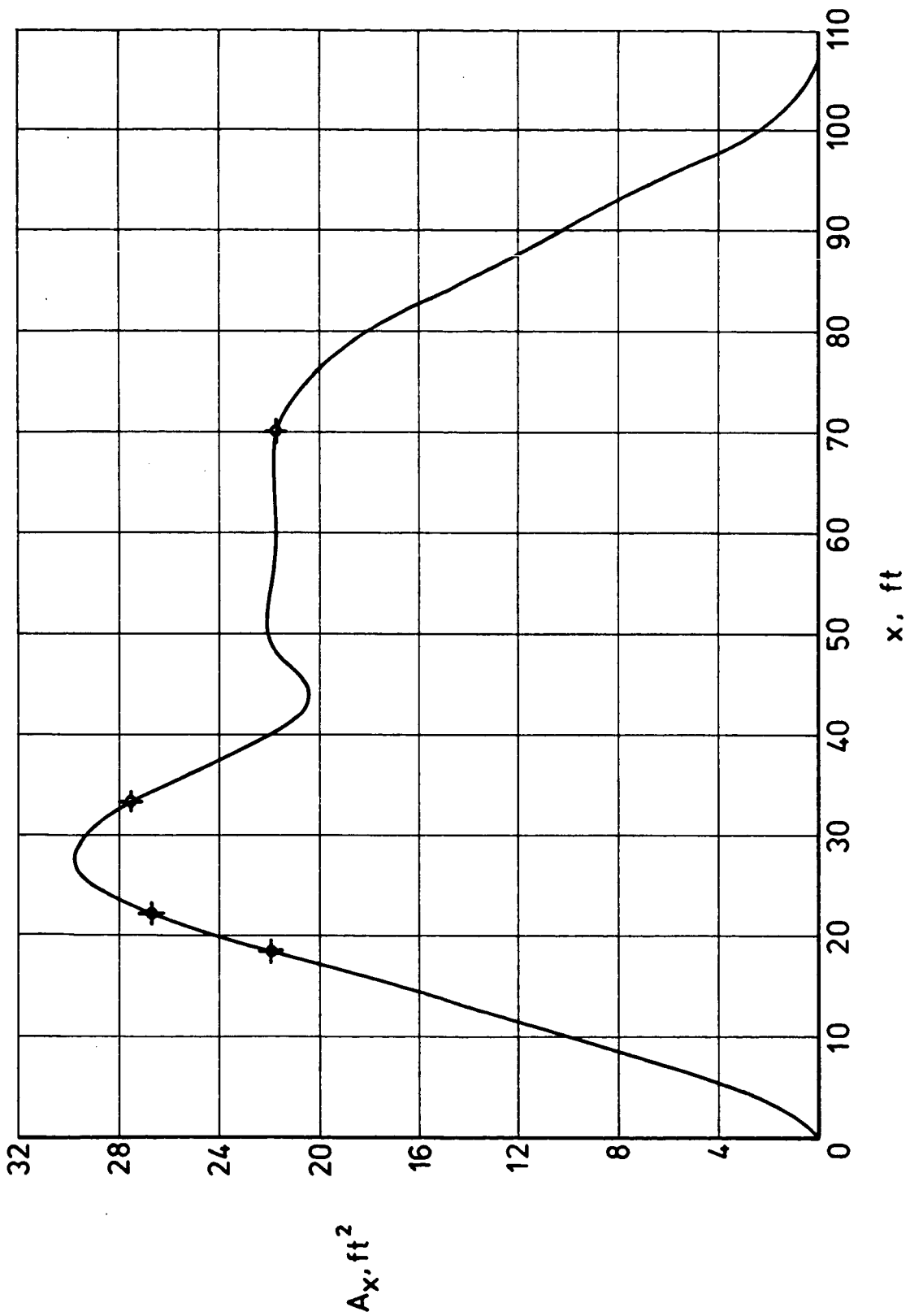


Figure I-6. - Fuselage normal cross-section area distribution optimized for  $M = 2$ .  
Constraint points indicated.

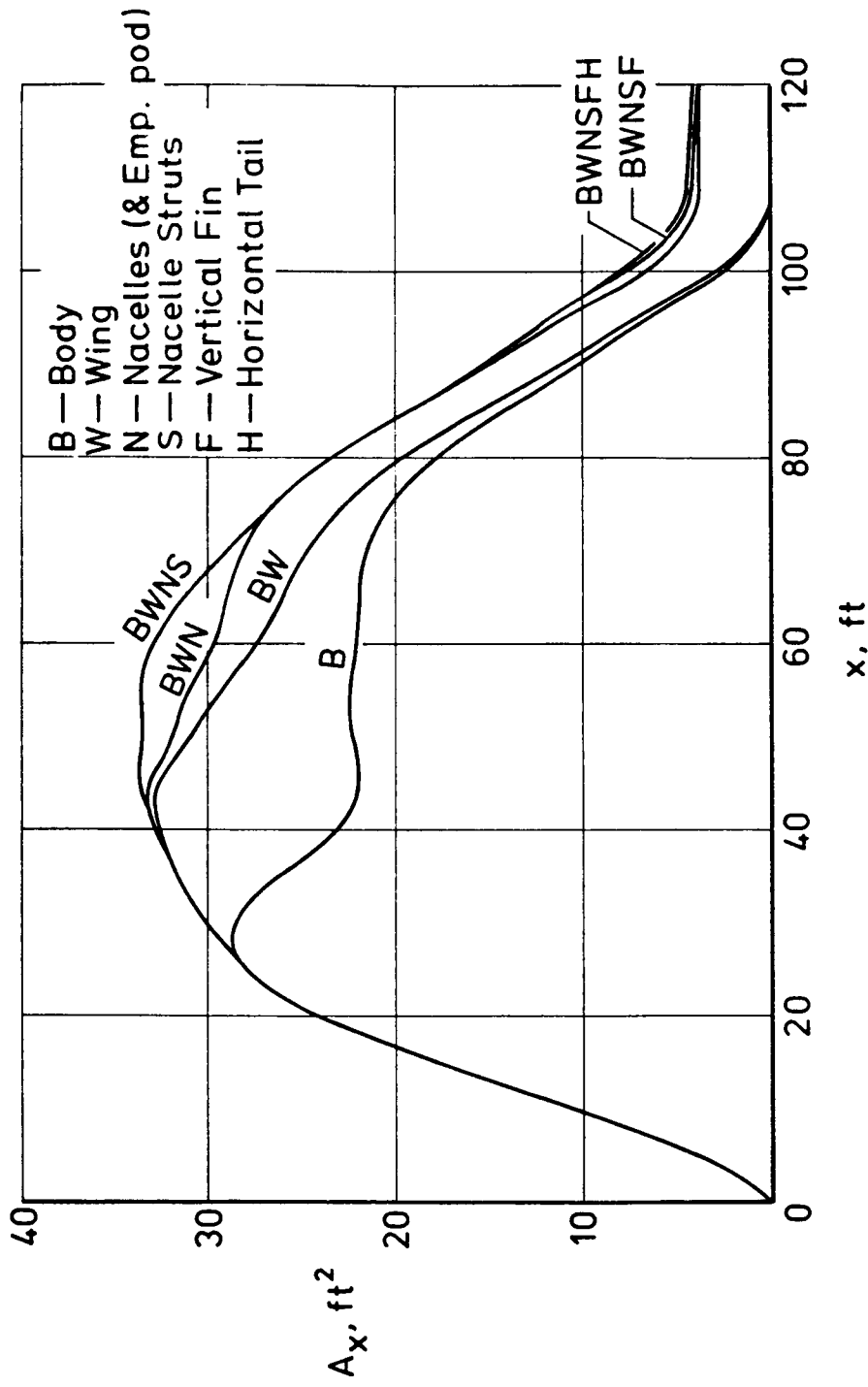


Figure I-7. - Average equivalent-body area distribution.  $M = 2.0$  condition.

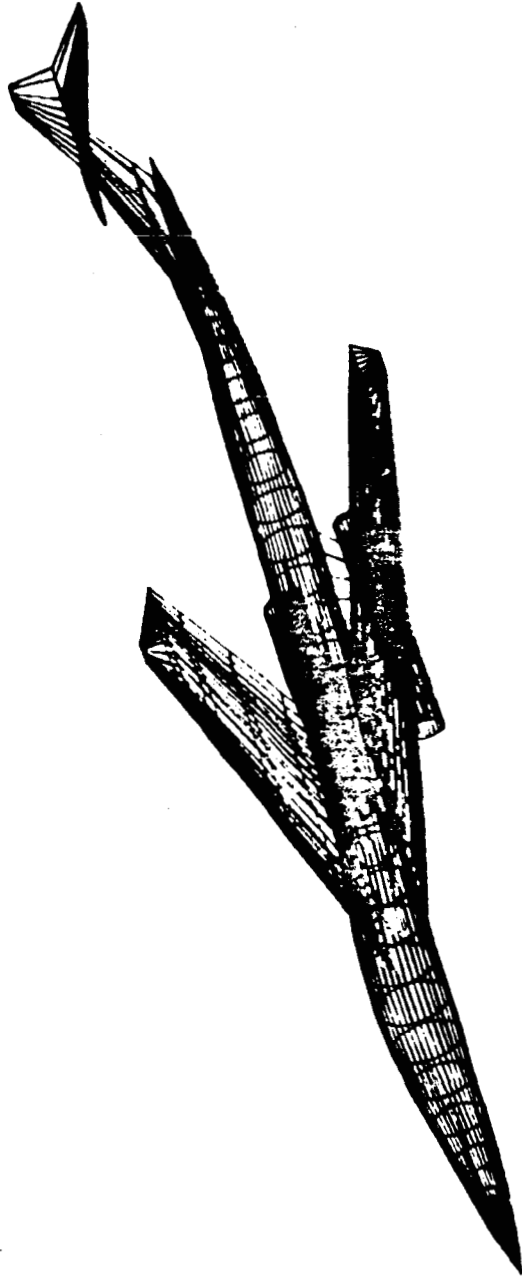


Figure I-8. - Computer drawing of numerical model of complete configuration.  
 $A_{LE} = 68^\circ$ .

## PART II. - CONFIGURATION DESCRIPTION

E. E. Swanson

The variable-sweep-wing concept has the same payload accommodations as those concepts studied in references 5 and 6 of the Introduction. Payload consists of 8 passengers and baggage with a flight crew of 2. Design range was targeted for approximately 3,500 nautical miles at a cruise speed of Mach 2.0. The passenger compartment cross section is similar in size to the Cessna Citation III. The arrangement, shown in figure II-1, has 2 three-place, divan-type seats facing the aircraft centerline with 2 single seats facing forward. The arrangement shown was selected to provide a minimum-length passenger compartment. Eight single-passenger seats could also be installed with reduced leg room based on light-weight airline type seats. A lavatory and a baggage area are provided aft of the passenger compartment. Approximately 50 cubic feet of space is allocated for passenger and crew baggage.

Weather radar and associated equipment is located in the nose section of the fuselage. Space allocation for the remaining subsystems, hydraulics, electrical, environmental control, and engine accessories, is provided aft of the baggage area as shown on figure II-1. Six fuel tanks are provided in the fuselage plus fuel in the wing box carry-through structure. Wing fuel consists of a triangular shaped tank forward of the wing pivot and outer wing fuel from the wing pivot to the tip between the front and rear spar.

A general arrangement and geometric characteristics of the study concept are presented in figure II-2 and table II-1, respectively. The fuselage is 107 feet long and the aircraft overall length is 114.42 feet. Wing span is 68.58 feet with the wings in the full forward sweep position and 40.39 feet in the full aft sweep position. A spanwise plot of streamwise thickness to chord ratio with the wing in the full aft sweep position is shown in figure II-3. Camber and thickness ordinates and planform details may be found in table I-1.

The engine used in this study is a modified version of a low bypass turbofan engine. Nacelle geometry is shown in figure II-4. The nacelles are mounted on struts cantilevered off of the fuselage below the wing. These same struts provide for mounting of the single strut dual wheel main landing gear which retracts into

the fuselage. The nose landing gear is a single wheel, single strut arrangement and retracts forward of the crew compartment into the aircraft nose, aft of the radar equipment.

In the previous supersonic business jet studies, a drooped visor nose was used to provide increased pilot vision during takeoff and landing. For this study concept, the nose camber of the fuselage was developed so that approximately 6 degrees of forward down vision are provided at the centerline of the pilots station with the aircraft at the static ground condition. In addition, during the landing approach condition, the aircraft attitude is approximately 6 degrees nose down from the normal cruise 1.0 g. flight condition. With these considerations, it was assumed that pilot vision would be adequate to safely operate the aircraft. Eliminating the visor nose saved approximately 250 - 300 pounds of structural and operating mechanism weight. Further design and simulator studies would be required to fully evaluate the feasibility of this concept.

TABLE II-I. - GEOMETRIC CHARACTERISTICS.

ITEM		WING	HORIZONTAL TAIL	VERTICAL TAIL
REFERENCE AREA, $S_{REF}$ , ft <sup>2</sup>		690.00	71.00	55.59
MAC (REF), $\bar{c}_{REF}$ , ft		19.79	7.03	9.68
SPAN, b	ft	37.00	11.30	9.68
ASPECT RATIO		1.984	1.800	.667
SWEEP, L.E., $\Lambda_{LE}$	deg	68	65	60
ROOT CHORD	ft	26.64	10.05	13.03
TIP CHORD	ft	10.66	2.51	5.21
ROOT t/c	%	4.667	2.996	2.996
TIP t/c	%	0	2.996	2.996
TAPER RATIO, $\lambda$		.40	.25	.40

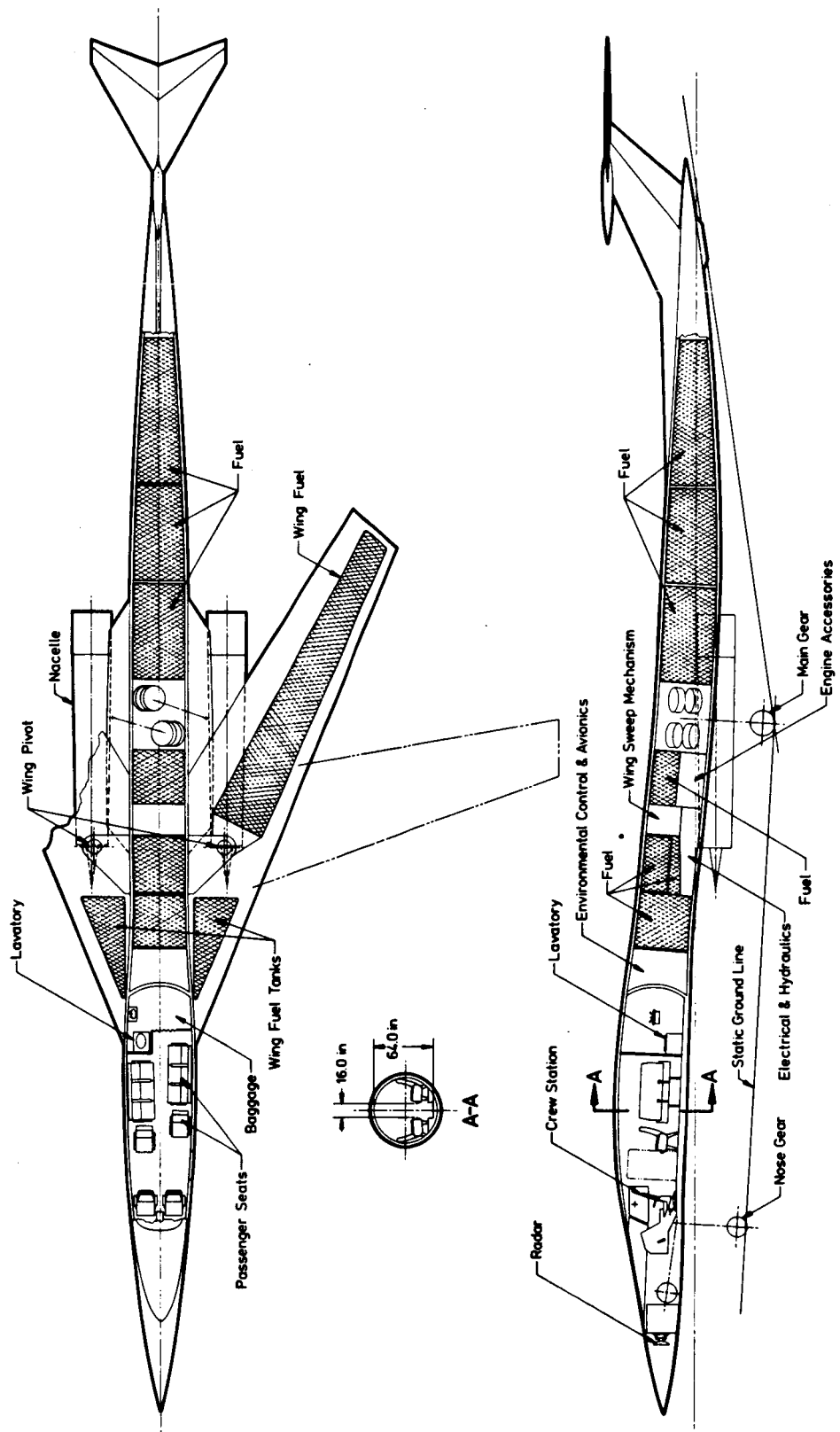


Figure II-1. - Interior arrangement.



Note:

All dimensions shown in feet unless otherwise specified.

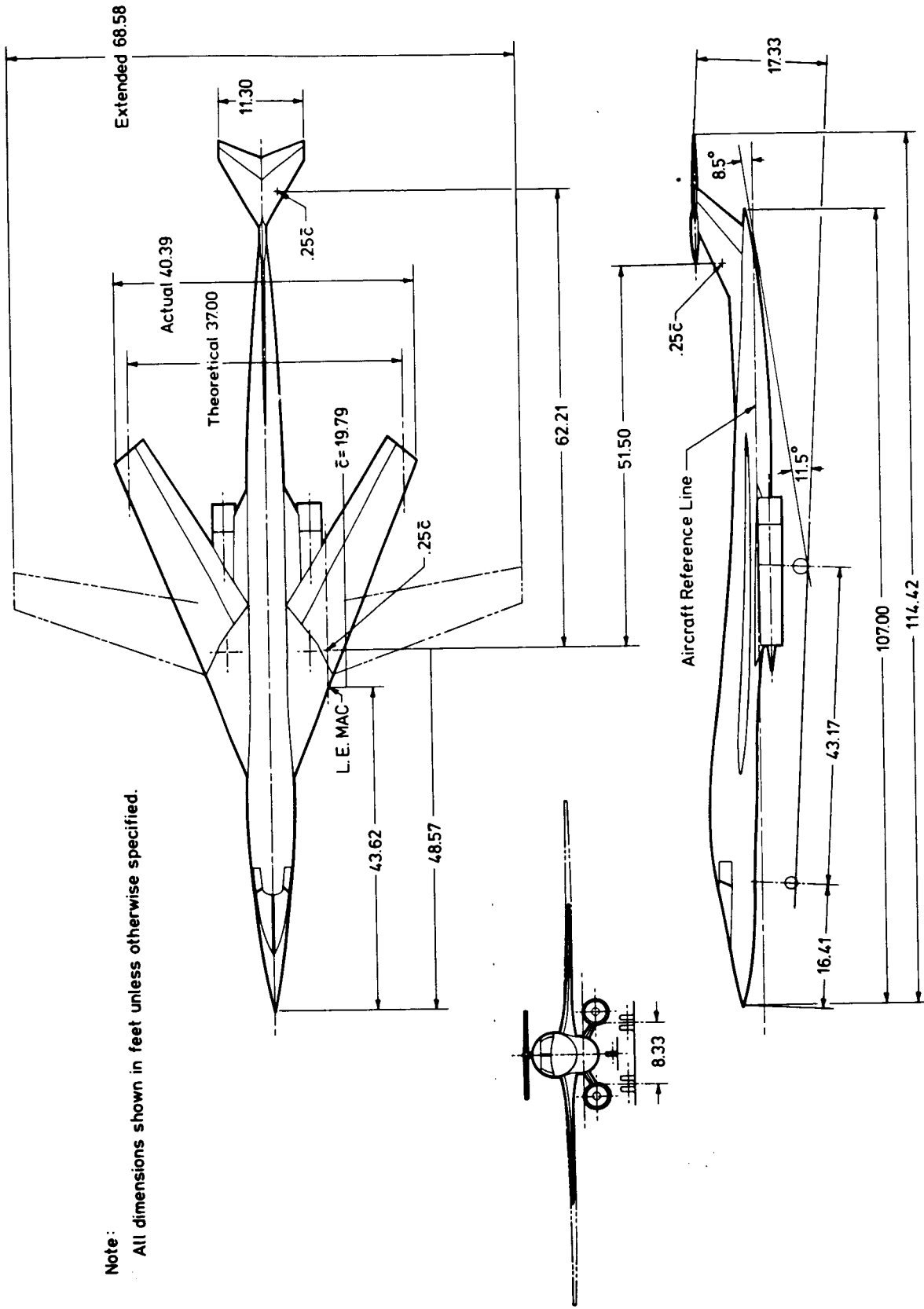


Figure II-2. - General arrangement.

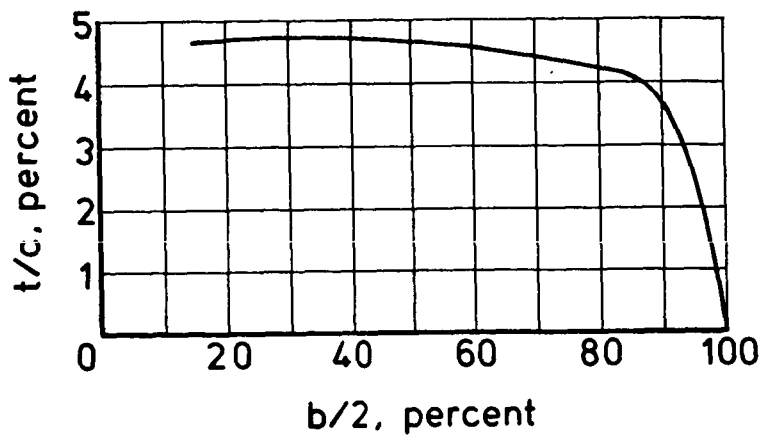


Figure II-3. - Wing spanwise thickness distribution. Full aft wing-sweep condition.

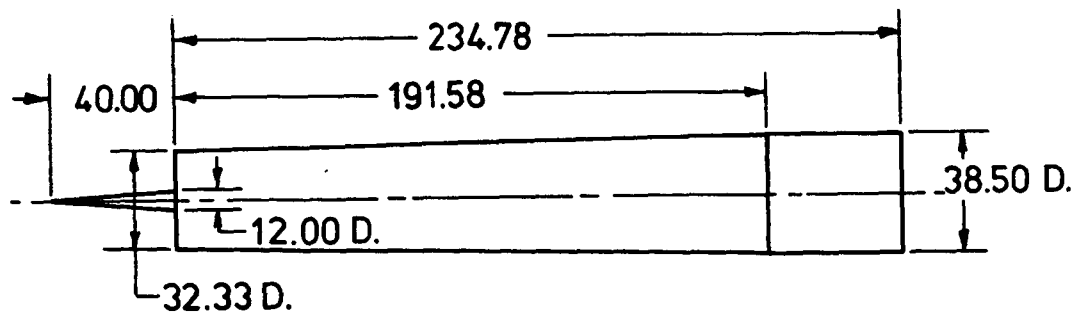


Figure II-4. - Nacelle geometry.

## PART III. - AERODYNAMICS

F. L. Beissner, Jr.

A. W. Robins

### Low-Speed Aerodynamics

The untrimmed lift curves and drag polars for the takeoff and landing configurations were predicted using the method of reference III-1 and are shown in figures III-1 and III-2. These predictions are based on full-span leading-edge slats and 85 percent span single-slotted, trailing-edge flaps. The takeoff and landing configuration leading-edge sweep was selected on the basis of stability considerations covered in Part I. Appropriate flap deflections were chosen to obtain the characteristic lift and drag curves.

### High-Speed Aerodynamics

Much of the methodology used to generate the high-speed aerodynamics of the configuration was discussed in Part I, which covered concept development. Drag items not discussed were skin friction, form, and roughness. Skin-friction drag values were found by the Sommer and Short T' method of reference III-2. Form drag is found by application of geometry-dependent factors of reference III-1 to the basic skin-friction values. Roughness drag was estimated from previously-developed empirical data. Figure III-3 provides a sample of these elements at the beginning of the tropopause (at  $h \approx 36,100$  feet) as well as the wave-drag contribution (discussed in Part I) to the buildup of zero-lift drag.

Drag due to lift was computed for the subsonic conditions by the methods of reference I-7 and reference III-3, and by the methods of references I-3 through I-6 for the supersonic conditions. Figure III-4 shows drag polars of the complete configuration at Mach numbers of 0.9 and 0.6 at wing sweeps of 35 and 20 degrees, respectively. Supersonic polars at Mach numbers of 2.0, 1.6, and 1.2 are shown in figure III-5 for the complete configuration at a wing sweep of 68 degrees.

Maximum attainable and operating lift-drag ratios are shown in figure III-6. These values are for the climb/cruise path of the design mission (see figure VI-1, Part VI).

## Sonic Boom

Sonic-boom overpressures were estimated using the simplified process described in reference III-4. Rather than use the simple shape-factor charts, however, equivalent cross-section areas due to both volume and lift were combined for six flight conditions to provide the characteristic shape factor for this specific study configuration. The results are shown in figure III-7, in which sonic-boom overpressures are plotted as a function of altitude and aircraft weight for Mach numbers of 1.2 and 2.0. The effects of various boom-alleviation flight profiles on both sonic boom and range are shown in the section covering aircraft performance.

## REFERENCES

- III-1. USAF Stability and Control DATCOM. Air Force Flight Dynamics Laboratory, Wright-Patterson Air Force Base, October 1960, revised April 1978.
- III-2. Sommer, Simon C.; and Short, Barbara J.: Free-Flight Measurements of Turbulent-Boundary-Layer Skin Friction in the Presence of Severe Aerodynamic Heating at Mach Numbers from 2.8 to 7.0. NASA TP 1500, 1979.
- III-3. Carlson, Harry W.; and Walkley, Kenneth B.: A Computer Program for Wing Subsonic Aerodynamic Performance Estimates Including Attainable Thrust and Vortex Lift Effects. NASA CR-3515, 1982.
- III-4. Carlson, Harry W.: Simplified Sonic Boom Prediction. NASA TP 1122, 1978.

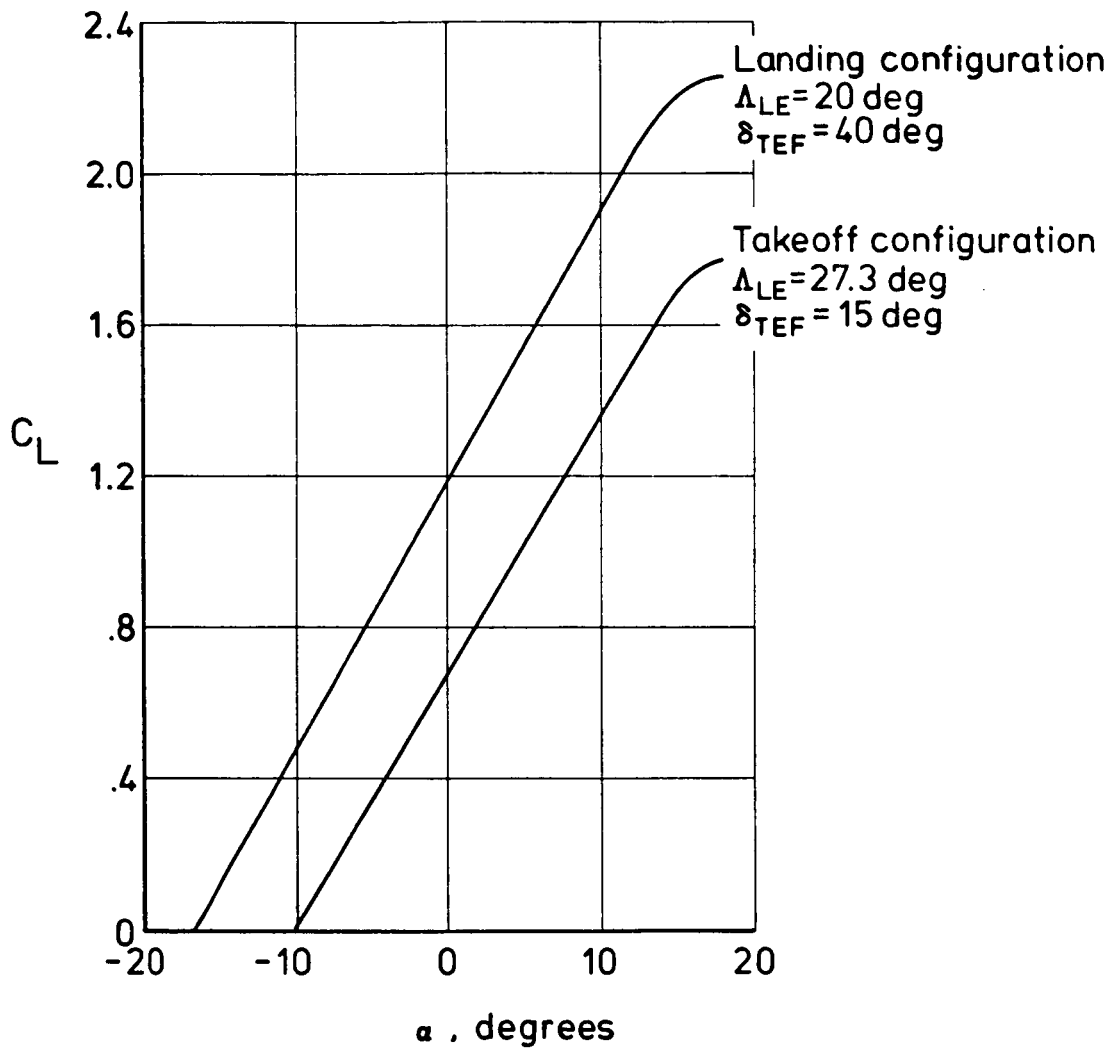


Figure III-1. - Low-speed lift for takeoff and landing. Out of ground effect; and untrimmed.  $M \approx 0.3$ .

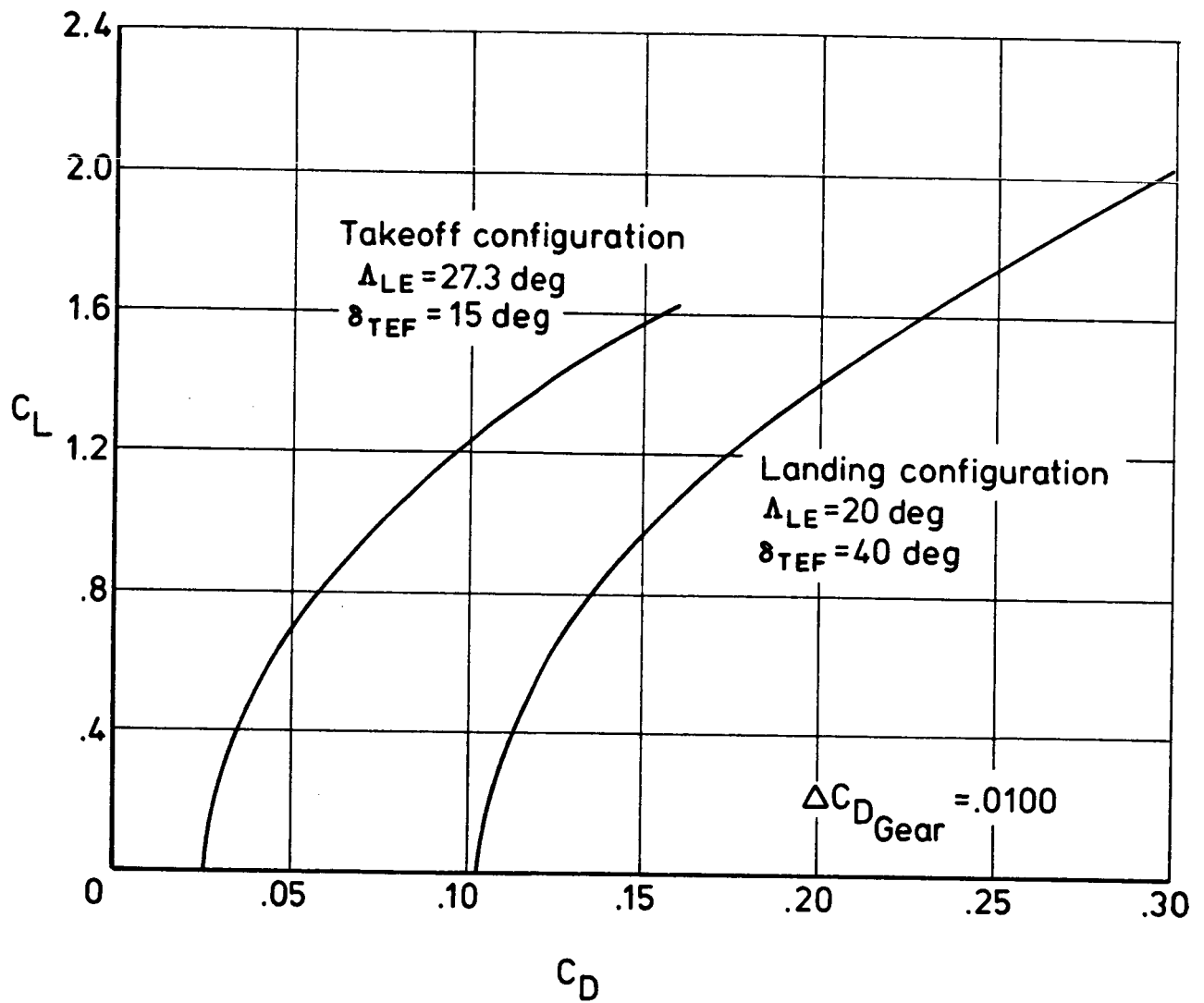


Figure III-2. - Drag polar for takeoff and landing. Out of ground effect; and untrimmed.  $M \approx 0.3$ .

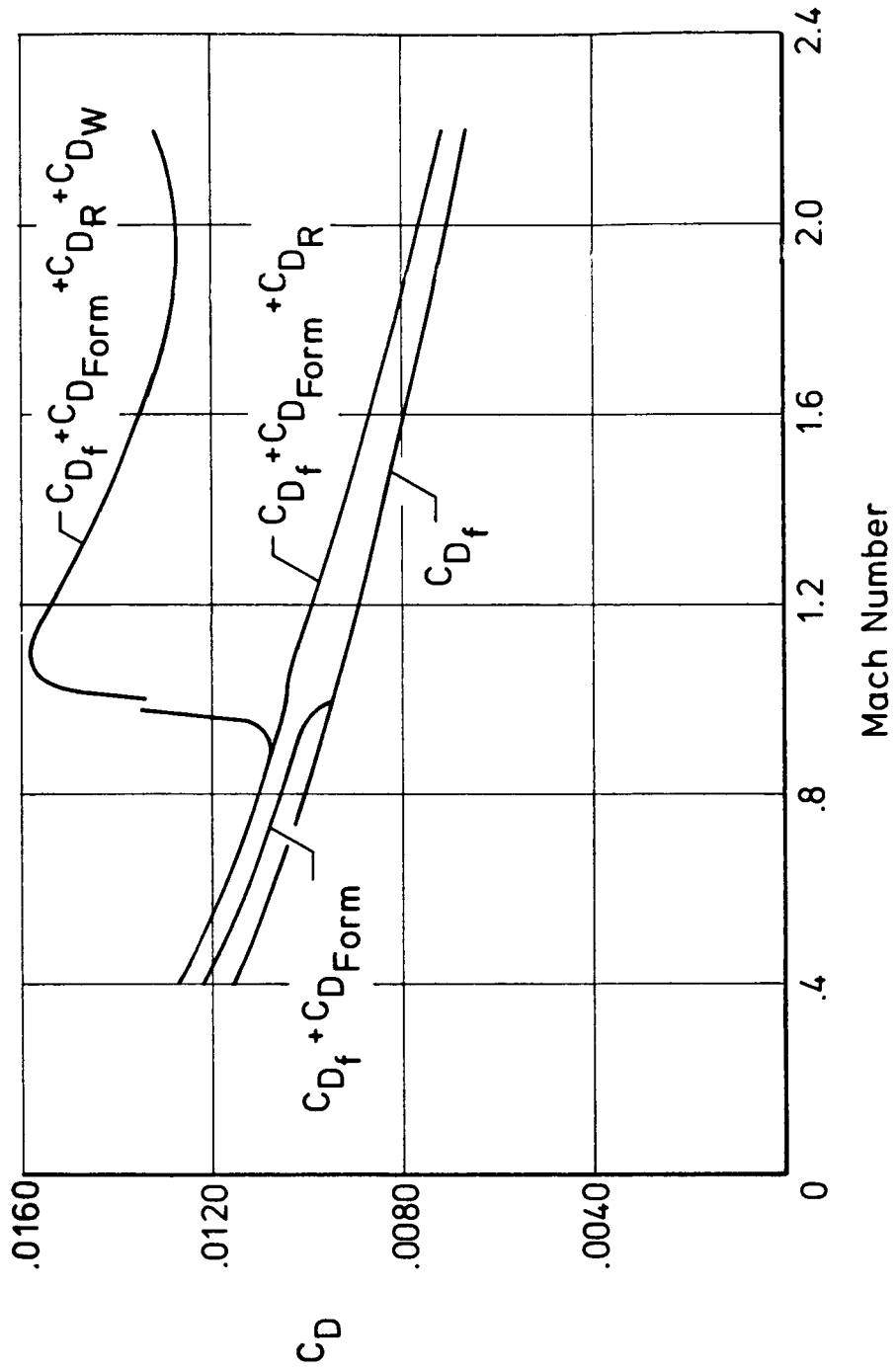


Figure III-3. - Buildup of zero-lift drag coefficient as a function of Mach number. Complete configuration with  $\Lambda_{LE} = 27.3^\circ$  at  $M < 1$  and  $\Lambda_{LE} = 68^\circ$  at  $M > 1$ .  $h = 36,1000$  feet.

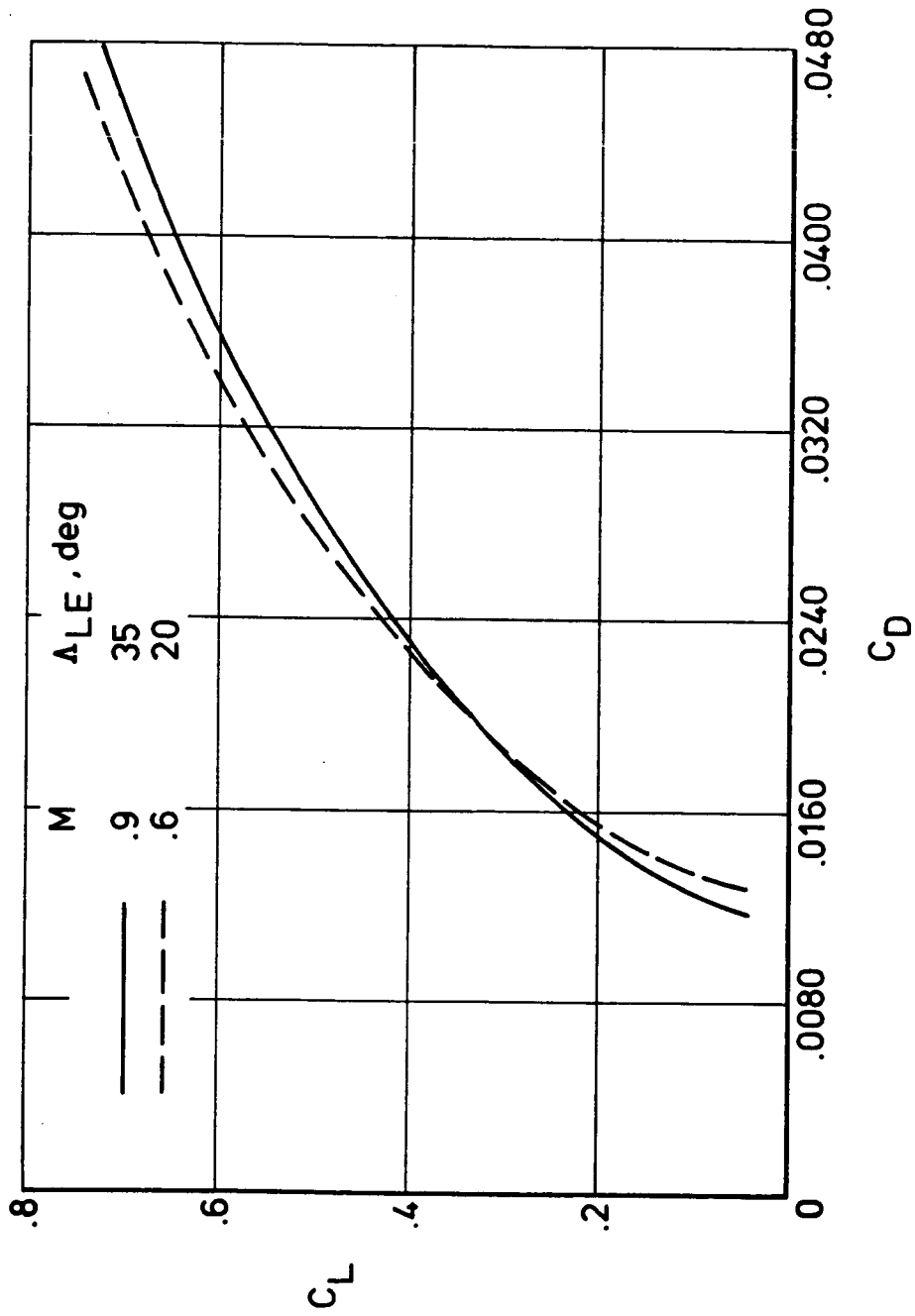


Figure III-4. - Subsonic drag polars. Complete configuration with  $\delta_F = 0$ .  $h = 36,100$  feet.



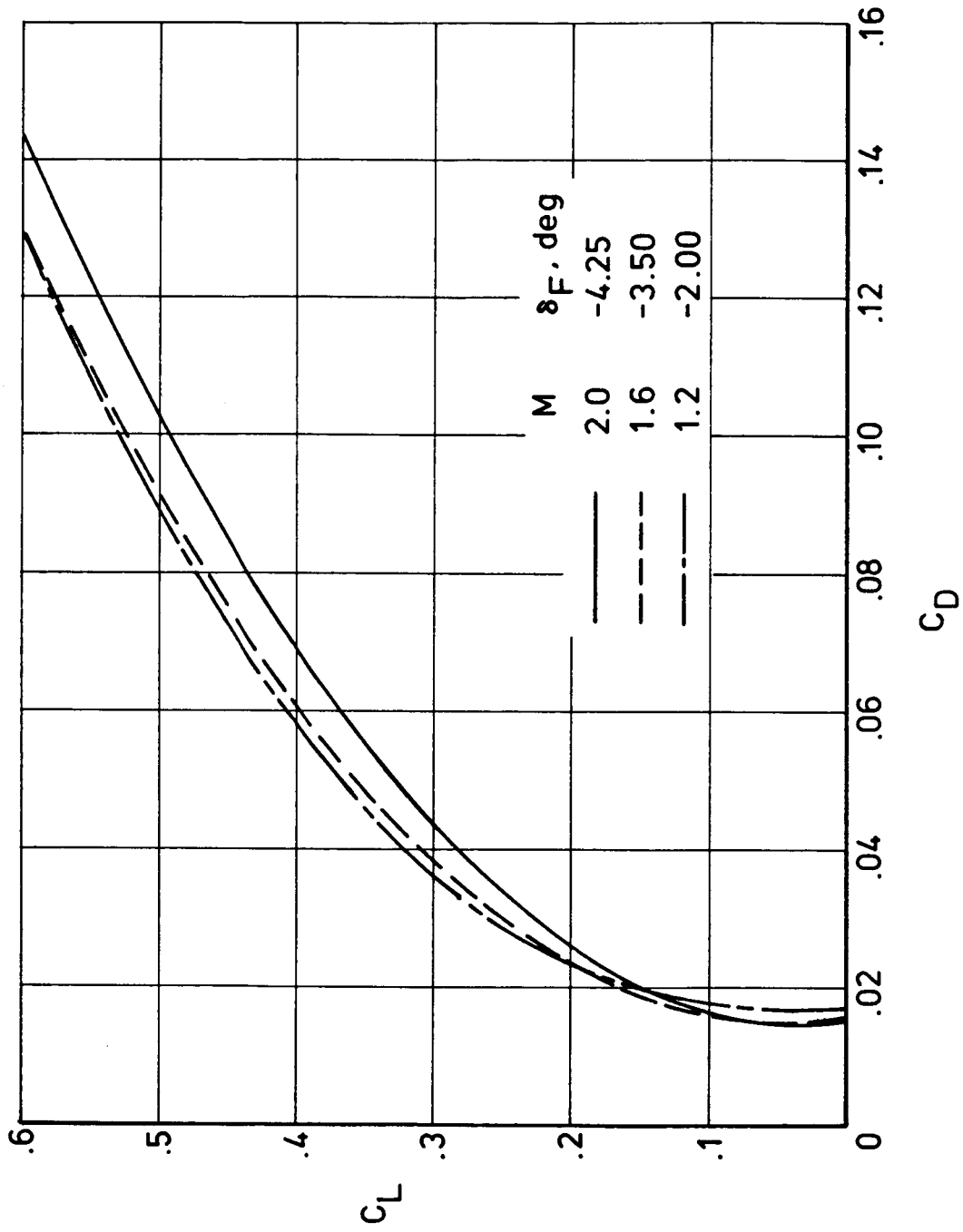


Figure III-5. - Supersonic drag polars. Complete configuration with  $\Lambda_{LE} = 68^\circ$  and  $\delta_H = 0^\circ$ .  
 $h = 36,100$  feet.

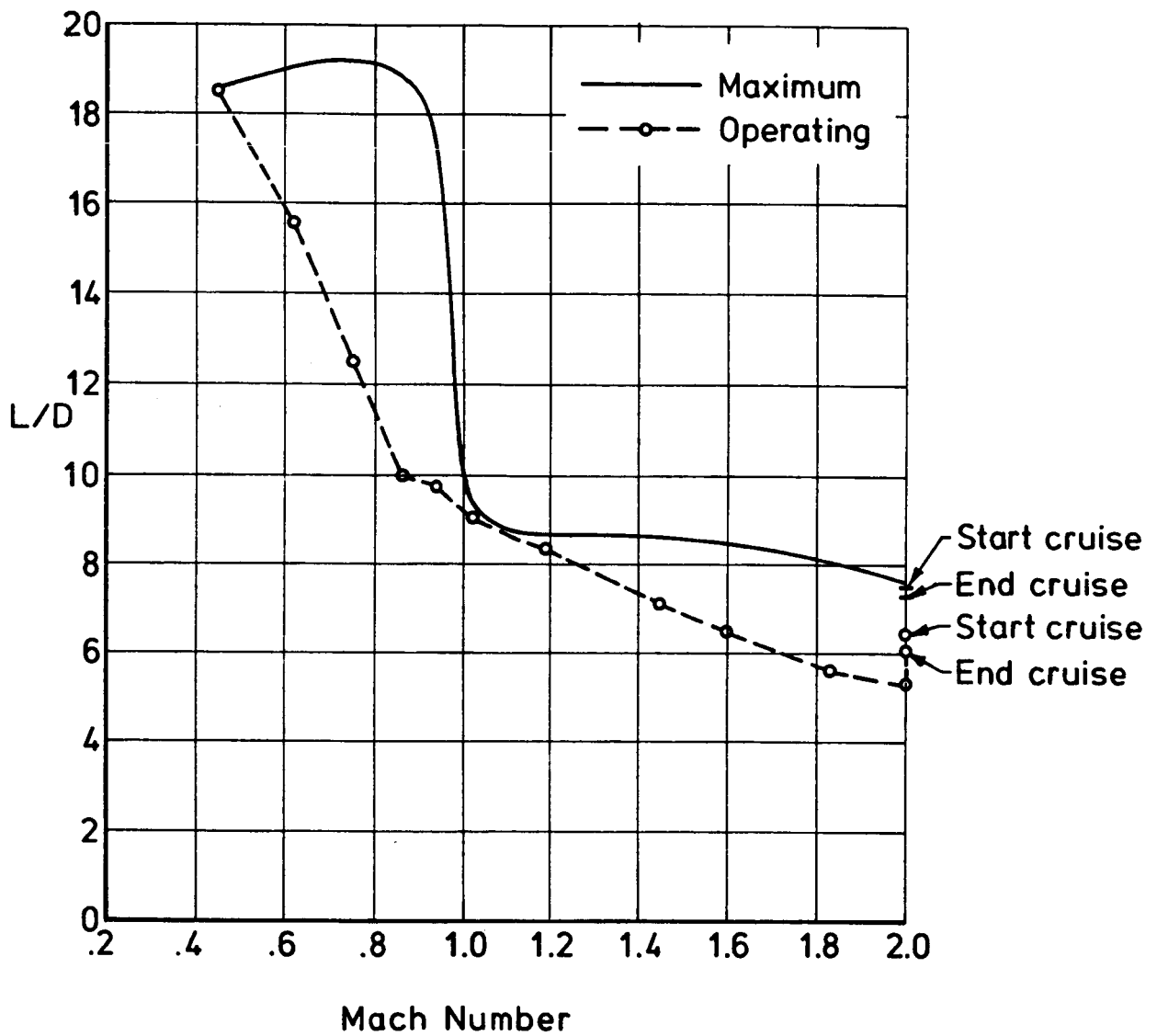
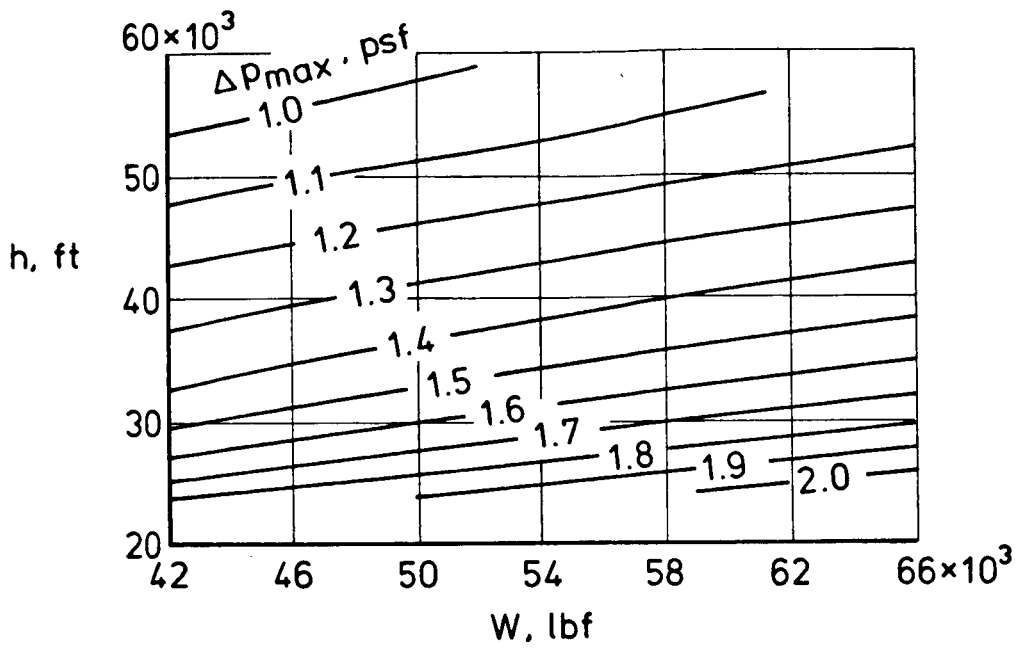
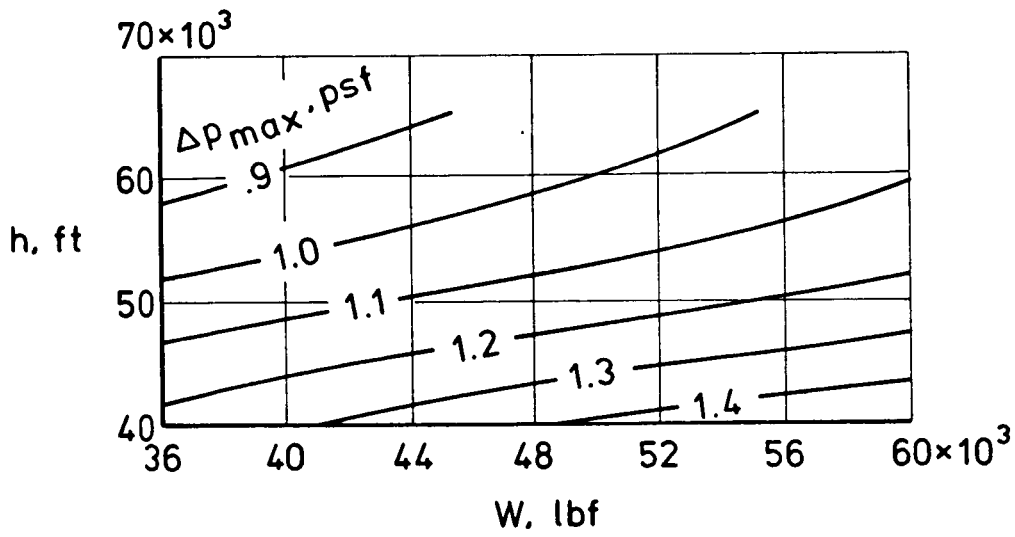


Figure III-6. - Maximum and operating lift-drag ratios along the climb/cruise path of the design mission.



(a)  $M=1.2$



(b)  $M=2.0$

Figure III-7. - Transonic and supersonic-cruise sonic-boom overpressures as a function of altitude and aircraft weight.

## PART IV. - PROPULSION

W. A. Lovell

The engine used in this study is a modified current-technology engine and was assumed to have an upper operational limit of Mach 2.4 at an altitude of 70000 feet at standard day atmospheric conditions. The current-technology engine data were modified based on anticipated technology advances and the potential for increasing the supersonic propulsive efficiency by modification of the fan and low pressure turbine. These modifications were estimated to have the potential to reduce the supersonic specific fuel consumption by about 20 percent and the engine weight by about 3 percent. Engine performance has been adjusted for the effects of Military specification inlet pressure recovery but not for installation drag, power extraction or service airbleed. The data used in this study is, therefore, somewhat optimistic.

### Baseline Engine

The baseline (current-technology) engine is a two-spool, low-bypass-ratio, augmented turbofan engine. It has a 3-stage low compressor, 1-stage low rotor, 10-stage compressor, and a 2-stage-turbine high rotor. A full annular duct surrounds the basic gas generator and supplies cooling air to the augmentor and nozzle. The inlet guide vanes, located ahead of the low compressor, have a movable trailing edge to achieve variable airfoil camber. This improves the inlet distortion tolerance, low compressor efficiency and enhances the engine acceleration characteristics. The high compressor has variable stators to improve starting and high Mach number characteristics.

The engine's exhaust nozzle is a variable throat area, balanced flap, convergent-divergent design. Nozzle area ratio varies as a function of nozzle throat area, so that both the throat and exit areas are simultaneously near optimum throughout the operating range.

Baseline engine performance is based on the 1962 U. S. Standard Atmosphere and Military specification inlet recovery (MIL-E-5008C). Since no other installation effects were considered, the performance used in this study is optimistic.

Baseline (as designed) engine characteristics at maximum power (with augmentation), sea-level static and standard-day atmospheric conditions are tabulated below:

Total-engine corrected airflow rate	178 lbm/sec
Fuel lower-heating value	18,400 Btu/lbm
Net thrust	21,000 lbf
Net specific fuel consumption	1.82 lbm/hr/lbf
Bypass ratio	0.155
Weight (including nozzle but no thrust reverser)	2,840 lbf
Maximum envelope diameter	38.5 in
Length of engine plus nozzle	161.8 in

#### STUDY ENGINE

To estimate the potential of the study aircraft with an advanced engine, the baseline engine was modified. Net thrust (gross thrust minus ram drag) levels were increased by 20 percent at Mach number 1.4 and above with no change in fuel flow rate. Engine weight (including nozzle but no thrust reverser) has been reduced by 3 percent with no change in the exterior engine geometry. These changes would necessitate a modification to the low-pressure spool of the engine. That is, one of the three stages of the low-pressure compressor would be eliminated and the remaining two stages reduced in diameter to reduce the bypass ratio. Associated with these modifications would be the requirement to modify the low-pressure turbine so as to achieve the proper work balance between the turbine and compressor.

Subsonic performance of the engine would also be affected by this modification; however, it has been assumed (optimistically) that subsonic performance decrements could be offset by incorporating a turbine bypass in the engine.

On the basis of these modifications, the baseline engine weight of 2,840 lbf is reduced to 2,755 lbf. Each of these weights include the basic engine and nozzle; however, they do not include a thrust reverser.

To estimate the nacelle drag and weight of a nacelle for the study engine, the engine was fitted with a NASA/Ames "P" inlet sized to match the engine. This inlet is a typical axisymmetric mixed compression design with a translating center-body sized for supersonic cruise conditions. A nacelle concept layout to house the engine incorporating a NASA/Ames "P" inlet and a variable throat area balanced flap convergent-divergent nozzle is shown in Figure II-4.

Estimated standard-day engine performance, adequate for preliminary aircraft mission performance analysis, is provided. These data are presented on figures IV-1 through IV-5 for maximum augmented power, maximum non-augmented power, and maximum and part power ratings.

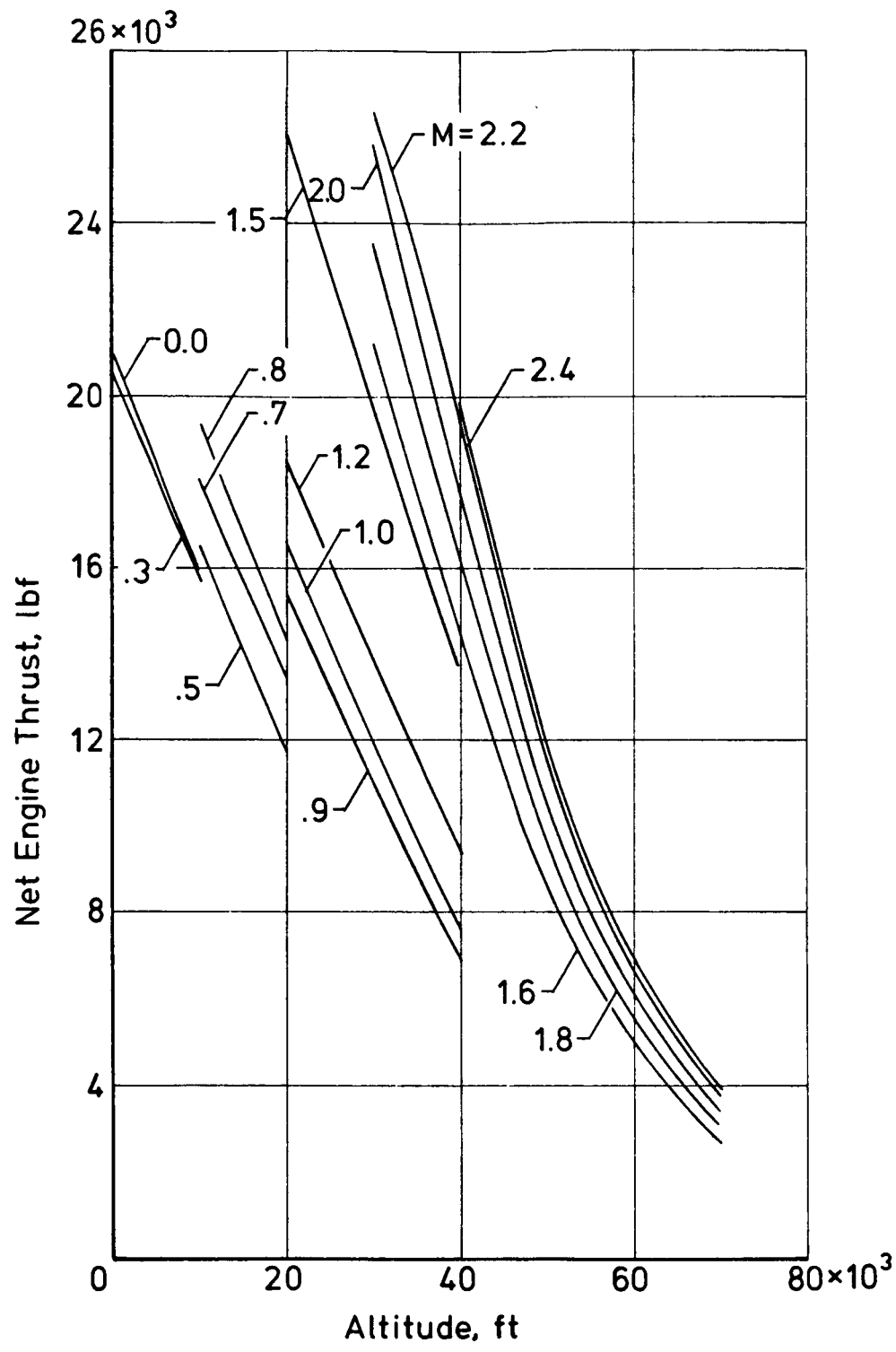


Figure IV-1. - Installed net engine maximum thrust. Standard-day conditions.

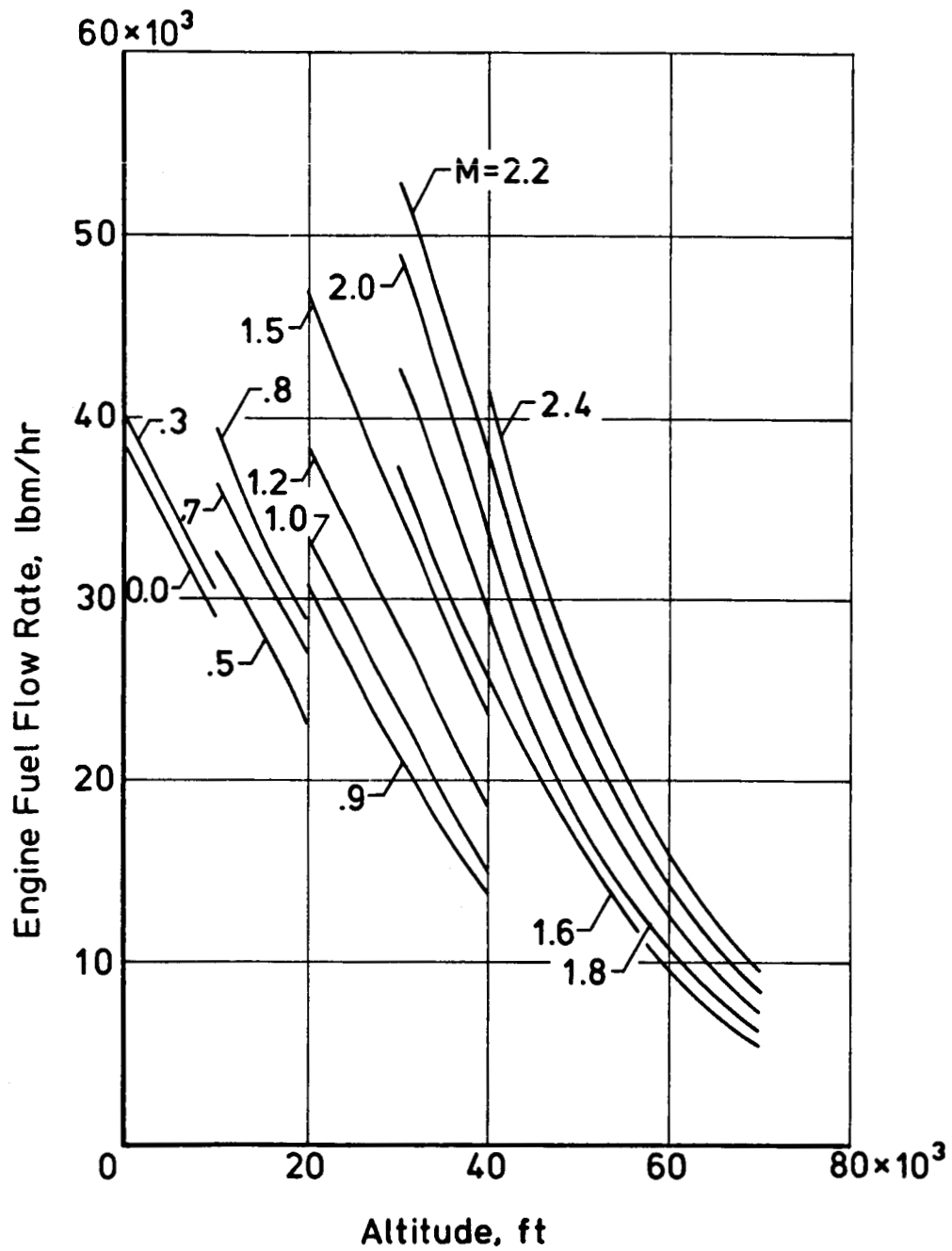


Figure IV-2. - Engine fuel-flow rate at maximum thrust. Standard-day conditions.



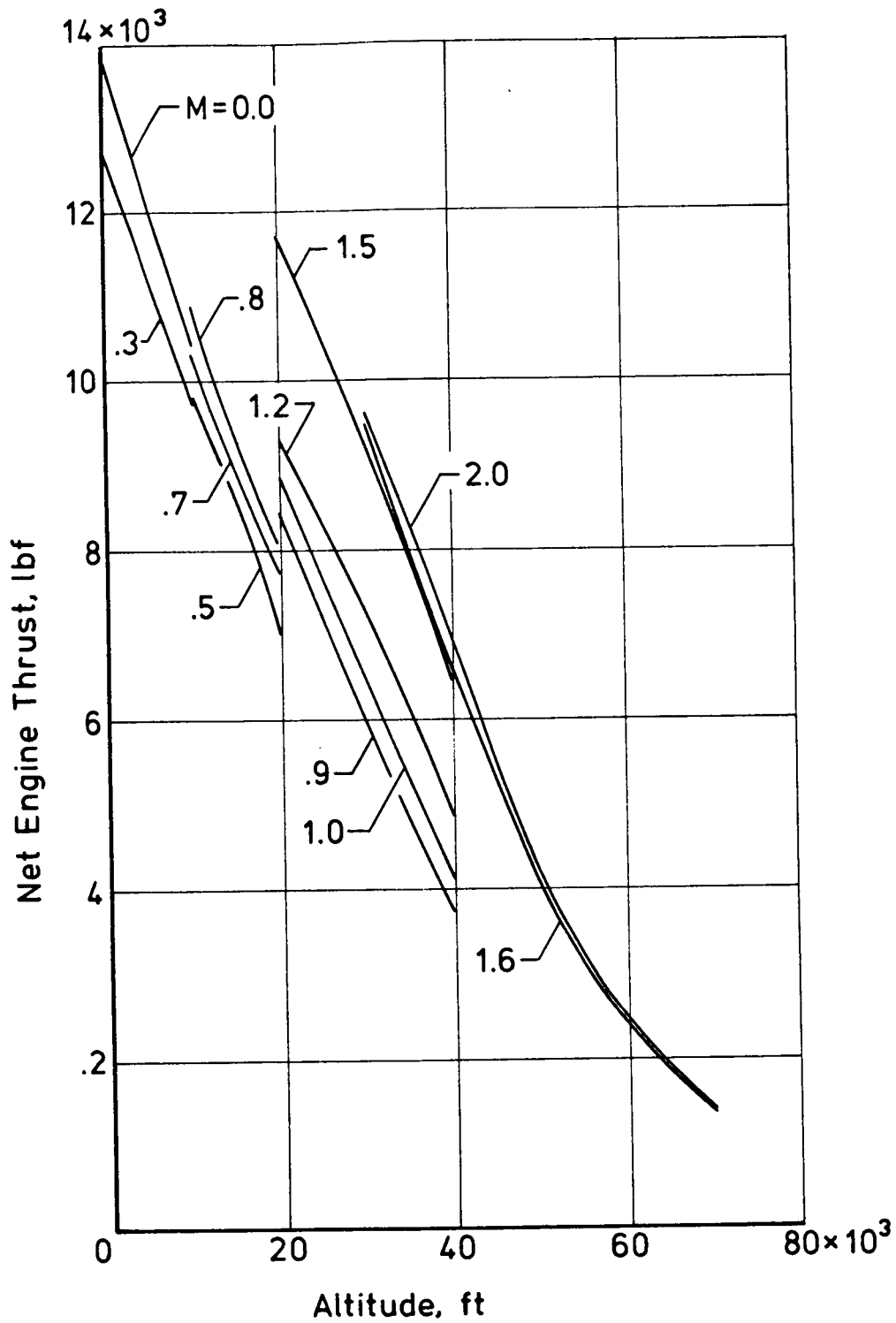


Figure IV-3. - Installed-engine intermediate thrust. Standard-day conditions.

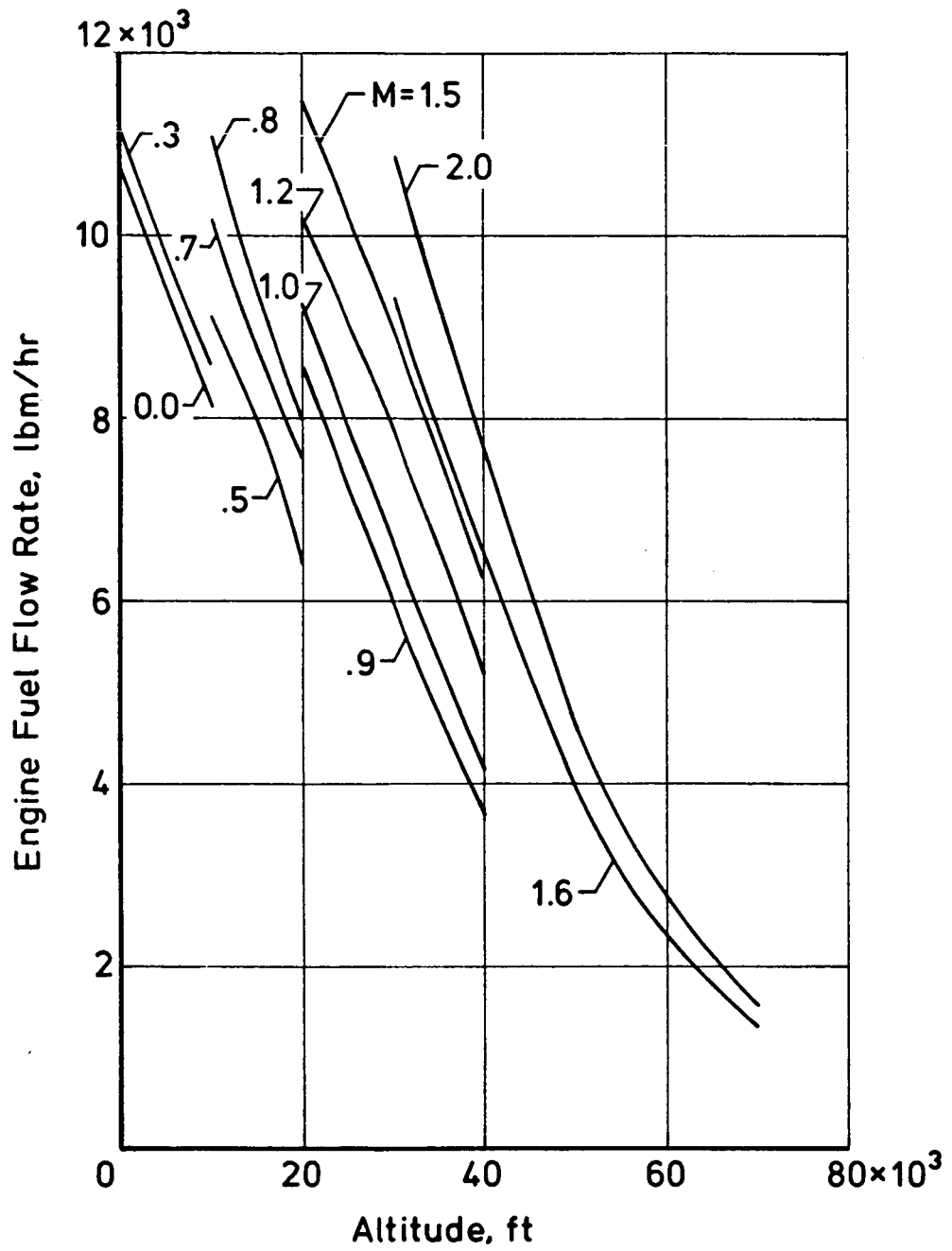


Figure IV-4. - Engine fuel-flow rate at intermediate thrust. Standard-day conditions.

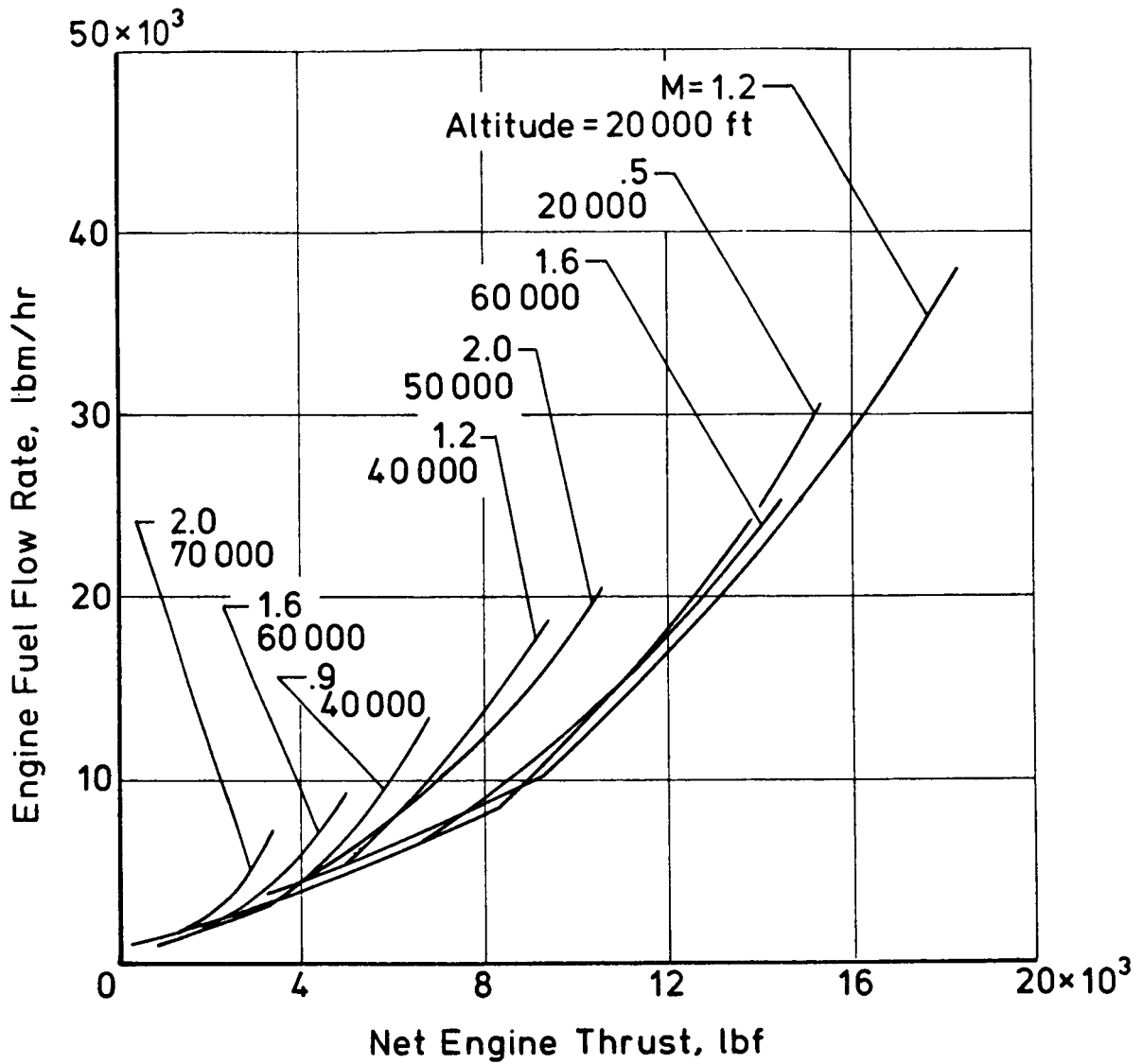


Figure IV-5. - Installed-engine fuel-flow rate for maximum acceleration and part-power thrust. Standard-day conditions.

## PART V. - MASS PROPERTIES

E. E. Swanson

The mass properties analysis for this configuration was performed using the weight module of the Flight Optimization System (FLOPS) computer program developed by Kentron Technical Center. A description of the program and its operating capabilities is described in the appendix of reference 6 of the Introduction. Structural weight estimates are based on utilizing 1980 technology superplastic formed/diffusion bonded (SPF/DB) titanium throughout all primary and secondary airframe structure. Applying this level of technology to the 1971 level of titanium structure results in the following anticipated weight saving:

Wing, empennage, etc.	-7%
Fuselage	-22%
Nacelle, inlet, cowling	-19%

In addition to the SPF/DB level of technology application, an all composite structural concept was evaluated. Previous studies have indicated that the application of composites to the fuselage pressure shell results in little or no weight reduction when compared to SPF/DB. It was assumed that the benefits of composites would, therefore, be assessed to the remaining structure and landing gear only. The following weight reductions were used for composites and were applied to the baseline concept instead of those listed above.

Wing, empennage, etc.	-15%
Surface controls	-12%
Nacelle, inlet, cowling	-25%
Landing gear	-40%
Fuselage (SPF/DB)	-22%

A detailed structural design and analysis of the wing pivot area was not performed during this study. Weight data from the F-111, F-14, and previous variable-sweep-wing supersonic-transport studies were analyzed and adjusted to reflect technology improvement in the pivot bearings and related structure. The resulting penalty of 17.5 percent for the pivot was applied to the wing weight. A three- to five-percent penalty was assessed to the weight of the hydraulics and

controls systems to account for the wing-sweep mechanism. The resulting weight breakdown for the SPF/DB and composite aircraft are shown in tables V-1 and V-2, respectively.

The center-of-gravity envelope for the wing in three sweep conditions is shown in figure I-3. Airplane inertias were not calculated during this study.

TABLE V-I. - GROUP WEIGHT SUMMARY

(SPF/DB Titanium)

	<u>lbf</u>
WING	6,647.
HORIZONTAL TAIL	427.
VERTICAL TAIL	308.
VERTICAL FIN	1,009.
FUSELAGE	4,651.
LANDING GEAR	1,669.
NACELLE	1,890.
STRUCTURE TOTAL	( 16,600.)
ENGINES	5,510.
MISCELLANEOUS SYSTEMS	388.
FUEL SYSTEM-TANKS AND PLUMBING	842.
PROPULSION TOTAL	( 6,740.)
SURFACE CONTROLS	1,626.
INSTRUMENTS	150.
HYDRAULICS	516.
ELECTRICAL	1,440.
AVIONICS	500.
FURNISHINGS AND EQUIPMENT	980.
AIR CONDITIONING	649.
ANTI-ICING	111.
SYSTEMS AND EQUIPMENT TOTAL	( 5,972.)
WEIGHT EMPTY	29,312.
CREW AND BAGGAGE - FLIGHT, 2	450.
UNUSABLE FUEL	321.
ENGINE OIL	131.
PASSENGER SERVICE	103.
OPERATING WEIGHT	30,317.
PASSENGERS, 8	1,320.
PASSENGER BAGGAGE	352.
ZERO FUEL WEIGHT	31,989.
MISSION FUEL	32,511.
TAKE-OFF GROSS WEIGHT	64,500.

## TABLE V-II. - GROUP WEIGHT SUMMARY

(All Composite)

	<u>lbf</u>
WING	4,637.
HORIZONTAL TAIL	359.
VERTICAL TAIL	259.
VERTICAL FIN	807.
FUSELAGE	4,651.
LANDING GEAR	1,012.
NACELLE	1,512.
STRUCTURE TOTAL	( 13,237.)
ENGINES	5,510.
MISCELLANEOUS SYSTEMS	388.
FUEL SYSTEM-TANKS AND PLUMBING	842.
PROPULSION TOTAL	( 6,740.)
SURFACE CONTROLS	1,406.
INSTRUMENTS	150.
HYDRAULICS	516.
ELECTRICAL	1,440.
AVIONICS	500.
FURNISHINGS AND EQUIPMENT	980.
AIR CONDITIONING	649.
ANTI-ICING	111.
SYSTEMS AND EQUIPMENT TOTAL	( 5,752.)
WEIGHT EMPTY	25,729.
CREW AND BAGGAGE - FLIGHT, 2	450.
UNUSABLE FUEL	321.
ENGINE OIL	131.
PASSENGER SERVICE	103.
OPERATING WEIGHT	26,734.
PASSENGERS, 8	1,320.
PASSENGER BAGGAGE	352.
ZERO FUEL WEIGHT	28,406.
MISSION FUEL	32,519.
TAKE-OFF GROSS WEIGHT	60,925.

## PART VI. - PERFORMANCE

F. L. Beissner, Jr.

Bringing together recent advances in several disciplines in a variable-sweep, supersonic-cruise executive jet has resulted in an aircraft with impressive performance and operational flexibility. The study objective was to utilize these advances to design a minimum size eight-passenger aircraft capable of meeting the design goal of supersonic transatlantic range.

The design aircraft with full internal fuel is capable of a supersonic mission of 3,477 n.mi. with 32,511 lbf fuel at a full up ramp weight of 64,500 lbf. Table VI-I and figure VI-1 show the mission performance summary and profile. Cruise is at  $M = 2.0$  with full payload of 8 passengers and a crew of 2. The baseline superplastic-formed/diffusion bonded (SPF/DB) titanium aircraft can be further improved by using advanced composites on the same geometric configuration to achieve a range of 3,737 n.mi. at a full up ramp weight of 60,925 lbf. This range improvement is all due to weight improvement. This mission is shown in table VI-II.

Mission performance is calculated for a main segment and a reserve segment. The main segment includes taxi-out and takeoff allowances (10 minutes fuel flow at idle power setting and 1 minute fuel flow at takeoff power setting), FAA climb ( $V \leq 250$  KCAS up to 10,000 ft altitude), climb and accelerate to start of cruise, cruise climb at cruise Mach number, and descent to destination. Reserves are included which provide for flight continuation to an alternate airport including missed-approach allowance (1 minute fuel flow at takeoff power setting), climb, subsonic cruise at 30,000 ft, hold for 30 minutes, and descent to the alternate airport. The alternate is located 250 n.mi. from the destination. All performance is for standard day, no wind conditions with no additional conservatism included. The performance is calculated by the Flight Optimization System (FLOPS) computer program described in reference 6 of the Introduction.

Performance was calculated for a subsonic cruise Mach number of 0.9. Using the same basic mission rules, the maximum range for the composite aircraft is 5,584 n.mi. at 60,925 lbf ramp weight. The SPF/DB airplane achieves 5,161 n.mi. These



missions are summarized in tables VI-III and VI-IV. This off-design range capability demonstrates the mission flexibility of the aircraft.

Emergency loss of an engine presents no range problem for this aircraft. Operation would be restricted to subsonic speeds, but the  $M = 0.9$ , engine-out range capability is nearly as good as the  $M = 0.9$ , two-engine range (and considerably better than the supersonic range). The worst possible case would be the loss of an engine at mid-mission on the maximum-range, subsonic mission. This worst case would require emergency use of a small portion of the planned reserves to reach the destination.

Alternate missions for the composite aircraft include the New York to Los Angeles route of 2,130 n.mi. This mission requires a minimum of 19,333 lbf of fuel for a ramp weight of 47,739 lbf as shown in table VI-V. The sonic-boom overpressure during acceleration for this case is 1.26 psf, a value which could be considered objectionable for normal overland operation of civil aircraft.

Some sonic-boom attenuation can be obtained by operating at higher altitudes than normal. For the study aircraft, by climbing (at subsonic speeds) to a higher-than-normal altitude before accelerating through the transonic speed zone, the overpressure can be reduced from 1.26 to 1.04 psf. This change in climb/acceleration schedule increases the fuel required for the mission by about 550 pounds and mission flight time is increased from 120 to 128 minutes due to substantially longer operating time at lower speeds during a much longer climb. Table VI-VI summarizes the sonic-boom attenuation study as applied to the New York to Los Angeles route.

Sonic boom is less of a problem for this aircraft at cruise conditions than during acceleration. For example, in the normal and boom attenuated climb schedules, the overpressures at the beginning of cruise are 1.02 and .99, respectively, and diminish as the flight continues. This information is included in table VI-VI. Calculation of the sonic boom characteristics for the study aircraft is covered in Part III of this report.

Airfield performance is outstanding with the wing unswept and the high-lift devices deflected. An intermediate power setting is more than ample with this aircraft/engine combination. Critical field length for the fully fueled, composite

aircraft is 4,600 ft with slats deflected, trailing-edge flaps deflected 15° and wing sweep set at 27.3°. Normal, two-engine takeoff distance is 3,300 ft over a 35 ft obstacle. Landing field length over a 50 ft obstacle at a landing weight of 44,247 lbf is 4,315 ft with slats, trailing edge flaps deflected 40°, and wing sweep of 20°. These distances are the computed values at sea-level, standard-day conditions with no conservatism included. Takeoff and landing lift curves and drag polars are shown in Part III.

Noise analyses were not performed in this preliminary design effort. Low power settings, low speeds, high lift coefficients, and high lift/drag ratios should provide a relatively benign airport noise environment. Calculations indicate that takeoff/climb-out performance would achieve over 5,400 ft altitude after traveling 3 n.mi. from brake release. Airfield performance is summarized in table VI-VII.

Alternate propulsion systems were evaluated in an earlier phase of this study. These were an advanced cycle (turbine by-pass turbojet) scaleable Boeing 701S engine (ref. VI-1) and two fixed size engines by General Electric, the GE F101 DFE and the GE F404 (data supplied by NASA). A comparison was made of mission range capability at the full fuel load for the then current configuration under consistent ground rules. Takeoff power was set to achieve the same approximate thrust level for comparable airfield performance. The advanced-cycle engine was sized to give maximum range with sufficient takeoff thrust. Compared to the other engines, the GE DFE was considerably heavier, and was also significantly poorer in mission performance. No further adjustments were attempted since the GE DFE was judged to be inferior for this particular application.

Table VI-VIII shows the tabular results of the comparison including some specific performance values. One of the candidate engines, the GE F404, had to be operated at maximum thrust at takeoff to achieve the desired thrust values. Examination of table VI-VIII shows that on the basis of supersonic mission range, the proper engine choice was the engine described in Part V of this report.

## REFERENCES

- VI-1. Fransicus, L. C.: Turbine Bypass Engine - A New Supersonic Cruise Propulsion Concept. NASA TM 82608, July 1981.

TABLE VI-I. - MISSION PERFORMANCE SUMMARY

DESIGN MISSION - SPF/DB AIRCRAFT

	WEIGHT (lbf)	FUEL (lbf)	DISTANCE (n.m.i.)	TIME (min.)	ALTITUDE (ft)	L/D	WT/SREF (lbf/ft <sup>2</sup> )
RAMP WEIGHT	64,500.						
TAXI OUT		371.		10.			
TAKEOFF WEIGHT	64,129.				-SEA LEVEL-		
TAKEOFF		357.		1.			
START CLIMB WEIGHT	63,772.						
CLIMB		3,094.	84.8	8.			
START CRUISE WEIGHT	60,678.				47,970.	6.43	87.9
CRUISE		24,460.	3,266.1	171.			
END CRUISE WEIGHT	36,218.				58,098.	6.10	52.5
DESCENT		269.	126.5	11.			
END DESCENT WEIGHT	35,949.						
RESERVE		3,960.					
ZERO FUEL WEIGHT	31,989.						
TAXI IN		371.		10.			
TOTAL FUEL		<u>32,511.</u>					
DESIGN RANGE			3,477.3				
FLIGHT TIME				190.			

BLOCK TIME = 3.52 HOURS  
 BLOCK FUEL = 28,922. POUNDS

TABLE VI-II. - MISSION PERFORMANCE SUMMARY

DESIGN MISSION - COMPOSITE AIRCRAFT

	WEIGHT (lbf)	FUEL (lbf)	DISTANCE (n.mi.)	TIME (min.)	ALTITUDE (ft)	L/D	WT/SREE <sub>2</sub> (lbf/ft <sup>2</sup> )
RAMP WEIGHT	60,925.						
TAXI OUT		371.		10.			
TAKEOFF WEIGHT	60,554.				-SEA LEVEL-		
TAKEOFF		357.		1.			
START CLIMB WEIGHT	60,197.						
CLIMB		2,965.	87.3	9.			
START CRUISE WEIGHT	57,232.				48,645.	6.32	82.9
CRUISE		24,690.	3,511.7	184.			
END CRUISE WEIGHT	32,542.				62,187.	6.31	47.2
DESCENT		270.	138.0	12.			
END DESCENT WEIGHT	32,272.						
RESERVE		3,866.					
ZERO FUEL WEIGHT	28,406.						
TAXI IN		371.		10.			
TOTAL FUEL		32,519.					
DESIGN RANGE			3,737.0				
FLIGHT TIME				204.			

BLOCK TIME = 3.76 HOURS  
 BLOCK FUEL = 29,024. POUNDS

TABLE VI-III. - MISSION PERFORMANCE SUMMARY

SUBSONIC MAXIMUM RANGE/COMPOSITE AIRCRAFT

	WEIGHT (lbf)	FUEL (lbf)	DISTANCE (n.mi.)	TIME (min.)	ALTITUDE (ft)	L/D	WT/SREF (lbf/ft <sup>2</sup> )
RAMP WEIGHT	60,925.						
TAXI OUT		371.		10.			
TAKEOFF WEIGHT	60,554.				-SEA LEVEL-		
TAKEOFF		357.		1.			
START CLIMB WEIGHT	60,197.						
CLIMB		1,548.	44.6	6.			
START CRUISE WEIGHT	58,648.				40,685.	16.96	85.0
CRUISE		26,134.	5,449.2	633.			
END CRUISE WEIGHT	32,515.				48,474.	16.10	47.1
DESCENT		246.	90.3	10.			
END DESCENT WEIGHT	32,268.						
RESERVE		3,862.					
ZERO FUEL WEIGHT	28,406.						
TAXI IN		371.		10.			
TOTAL FUEL		<u>32,519.</u>					
DESIGN RANGE			5,584.0				
FLIGHT TIME				649.			

BLOCK TIME = 11.16 HOURS  
 BLOCK FUEL = 29,028. POUNDS

TABLE VI-IV. - MISSION PERFORMANCE SUMMARY  
 SUBSONIC MAXIMUM RANGE - SPF/DB AIRPLANE

	WEIGHT (lbf)	FUEL (lbf)	DISTANCE (n.mi.)	TIME (min.)	ALTITUDE (ft)	L/D	WT/SREE (lbf/ft <sup>2</sup> )
RAMP WEIGHT	64,500.						
TAXI OUT		371.		10.			
TAKEOFF WEIGHT	64,129.				-SEA LEVEL-		
TAKEOFF		357.		1.			
START CLIMB WEIGHT	63,772.						
CLIMB		1,634.	46.2	6.			
START CRUISE WEIGHT	62,138.				40,002.	16.97	90.1
CRUISE		25,945.	5,024.1	584.			
END CRUISE WEIGHT	36,193.				47,455.	16.37	52.5
DESCENT		248.	90.9	9.			
END DESCENT WEIGHT	35,945.						
RESERVE		3,956.					
ZERO FUEL WEIGHT	31,989.						
TAXI IN		371.		10.			
TOTAL FUEL		<u>32,511.</u>					
DESIGN RANGE			5,161.2				
FLIGHT TIME				599.			

BLOCK TIME = 10.34 HOURS  
 BLOCK FUEL = 28,926. POUNDS

TABLE VI-V. - MISSION PERFORMANCE SUMMARY  
 MINIMUM FUEL M = 2.0 CRUISE NEW YORK TO LOS ANGELES - COMPOSITE AIRPLANE

	WEIGHT (lbf)	FUEL (lbf)	DISTANCE (n.mi.)	TIME (min.)	ALTITUDE (ft)	L/D	WT/SREF (lbf/ft <sup>2</sup> )
RAMP WEIGHT	47,739.						
TAXI OUT		371.		10.			
TAKEOFF WEIGHT	47,368.				-SEA LEVEL-		
TAKEOFF		357.		1.			
START CLIMB WEIGHT	47,011.						
CLIMB		2,386.	79.8	8.			
START CRUISE WEIGHT	44,625.				55,593.	6.46	64.7
CRUISE		12,082.	1,912.2	100.			
END CRUISE WEIGHT	32,543.				62,185.	6.31	47.2
DESCENT		270.	138.0	12.			
END DESCENT WEIGHT	32,273.						
RESERVE		3,867.					
ZERO FUEL WEIGHT	28,406.						
TAXI IN		371.					
TOTAL FUEL		19,333.					
DESIGN RANGE			2,130.0				
FLIGHT TIME				120.			

BLOCK TIME = 2.35 HOURS  
 BLOCK FUEL = 15,837. POUNDS



TABLE VI-VI. - SONIC BOOM STUDY SUMMARY  
 COMPOSITE AIRCRAFT, NEW YORK TO LOS ANGELES ROUTE, M = 2.0 CRUISE

Profile	Mimumum Fuel	Reduced Boom
Ramp weight, lbf	47,739	48,288
Mission fuel, lbf	19,333	19,882
Acceleration ( M = 1.2)		
Altitude, ft	41,000	52,500
Weight, lbf	45,700	44,700
Overpressure psf	1.26	1.04
Start cruise (M = 2.0)		
Altitude, ft	55,590	56,140
Weight, lbf	44,625	42,733
Overpressure, psf	1.02	.99

TABLE VI-VII. - AIRFIELD PERFORMANCE AND NOISE CHARACTERISTICS SUMMARY  
 COMPOSITE AIRCRAFT, FULL INTERNAL FUEL

$\delta_F$ TO/Land, Degrees	15/40
Landing, lbf	44,247
Field Length (50 Ft Obs), ft	4,313
Ground Roll, ft	3,201
$V_K$ (Obs)	118.88
Take Off, Lbf	60,925
Field Length (35 Ft Obs), ft	3,295
Ground Roll, ft	2,411
$V_K$ (Obs), Knots	165.60
Critical (Balanced) Field, ft	4,582
Noise Criteria	
Take Off (3 Miles From Brake Release)	
L/D	13.80
$C_L$	.7951
Altitude, ft	5,435
$V_K$ , Knots	173.97
Thrust, lbf*	25,615/8,830
Approach (3° Glide Slope)	
L/D	6.66
$C_L$	1.3336
$V_K$ , knots	118.88
Thrust, lbf	4,293

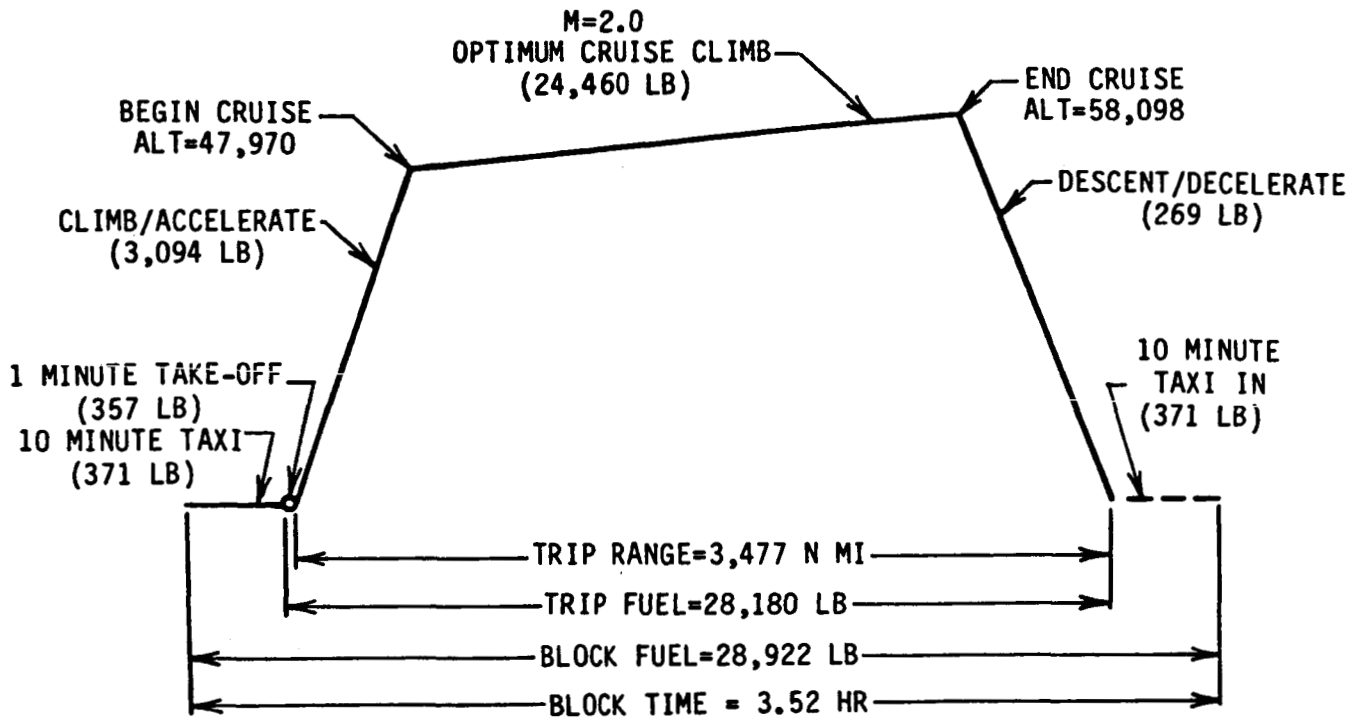
\*Thrust available before cutback/after cutback.

NOTE: All performance is at sea level, standard day conditions,  
 with no conservatism.

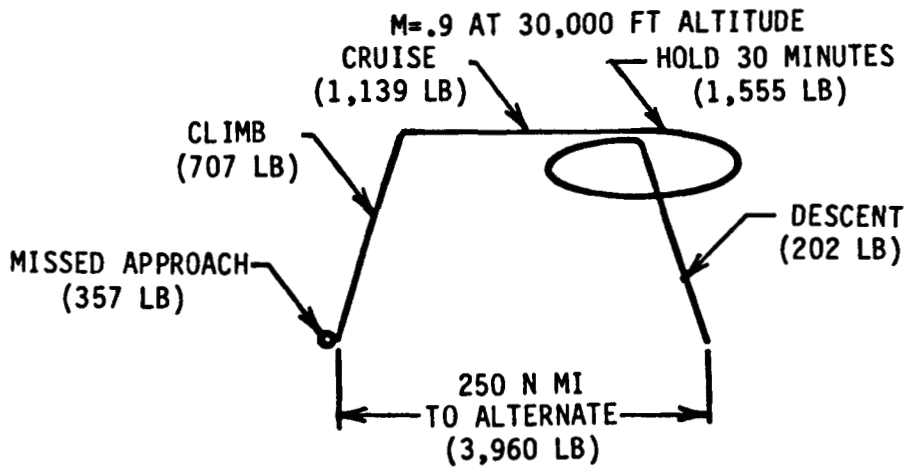
TABLE VI-VIII. - PROPULSION SYSTEM COMPARISON  
 PRELIMINARY CONFIGURATION, DESIGN MISSION, SAME AIRPLANE  
 (AERODYNAMICS, WEIGHT AND FUEL)

ENGINE DESIGNATION	BASELINE	BOE 701S	GE DFE	GE F404
ENGINE SIZE FACTOR	FIXED	.221	FIXED	FIXED
ENGINE WEIGHT, lbf, ea	2,755	2,873	4,258	2,621
TAKEOFF THRUST, lbf	13,785	14,940	14,550	14,200
POWER SETTING FOR TAKEOFF	INT	*	INT	MAX
TOTAL RANGE, n.mi.	3,364	3,074	2,419	2,630
AVERAGE CRUISE				
SPECIFIC RANGE, $V/w_f$ , nmi/lbm	.1254	.1227	.0909	.1038
SPECIFIC FUEL CONSUMPTION $\frac{lbm}{lbf \cdot hr}$	1.147	1.314	1.490	1.556
LIFT/DRAG	6.19	6.94	5.82	6.88
ALTITUDE, ft	53,367	59,618	51,208	59,646
WEIGHT, lbf	49,389	49,415	49,301	48,875
FUEL, lbf	9,152	9,353	12,625	11,056
TAXI ALLOWANCE, lbf	371	418	411	341
TAKEOFF ALLOWANCE, lbf	357	523	337	667
RESERVES, lbf	3,976	5,088	4,178	4,696

\*The Boeing 701S is not equipped with afterburner.



A. Main Segment.



B. Reserve Segment.

Figure VI-1. Design mission profile, titanium SPF/DB aircraft, M=2.0 cruise, full internal fuel.

1. Report No. NASA CR-172321		2. Government Accession No.		3. Recipient's Catalog No.	
4. Title and Subtitle Application of Near-Term Technology to a Mach 2.0 Variable-Sweep-Wing, Supersonic-Cruise Executive Jet				5. Report Date March 1984	
				6. Performing Organization Code	
7. Author(s) F. L. Beissner, Jr.; W. A. Lovell; A. Warner Robins; and E. E. Swanson				8. Performing Organization Report No.	
				10. Work Unit No.	
9. Performing Organization Name and Address Kentron International, Inc. Aerospace Technologies Division Hampton, VA 23666				11. Contract or Grant No. NAS1-16000	
				13. Type of Report and Period Covered Contractor Report	
12. Sponsoring Agency Name and Address National Aeronautics and Space Administration Washington, DC 20546				14. Sponsoring Agency Code 505-43-43-01	
15. Supplementary Notes  Langley Technical Monitor: Charles E. K. Morris, Jr.					
16. Abstract  An analytic study has been conducted to assess the impact of variable-sweep-wing technology with relaxed static stability requirements on a supersonic-cruise executive jet with transatlantic range. The baseline vehicle utilized modified, current-technology engines and titanium structures produced with superplastic forming and diffusion bonding; this vehicle meets study requirements for both supersonic-cruise and low-speed characteristics.  The baseline concept has a ramp weight of 64,500 pounds with a crew of two and eight passengers. Its Mach 2.0 cruise range is nearly 3,500 nautical miles; its Mach 0.9 cruise range is over 5,000 nautical miles. Takeoff, landing, and balanced field length requirements were calculated for a composite variant and are all less than 5,000 feet.					
17. Key Words (Suggested by Author(s)) Aircraft Configurations Supersonic Business Jet Variable Sweep			18. Distribution Statement  Unclassified - Unlimited  Star Category 05 - Aircraft Design, Testing and Performance		
19. Security Classif. (of this report) Unclassified		20. Security Classif. (of this page) Unclassified		21. No. of Pages 60	22. Price A04